

https://dspace.org/

Matching land surface phenology with the phenology of net ecosystem exchange (NEE) in the Kruger National Park, South Africa

Ngubane, Dalingcebo

2021

https://hdl.handle.net/10539/32472

Ngubane,Dalingcebo (2021) Matching land surface phenology with the phenology of net ecosystem exchange (NEE) in the Kruger National Park, South Africa, University of the Witwatersrand, Johannesburg, <http://hdl.handle.net/10539/32472>

Downloaded from a DSpace repository. https://dspace.org/



Matching land surface phenology with the phenology of net ecosystem exchange (NEE) in the Kruger National Park, South Africa.

by

Dalingcebo Ngubane

(867230)

Dissertation

Submitted in fulfilment of the requirements for the degree

Master of Science

in

Animal Plant and Environmental Science

in the Faculty of Science, University of the Witwatersrand, Johannesburg, South Africa

Supervisor: Dr. Yolandi Ernst

Co-supervisor: Prof. Francesca Parrini

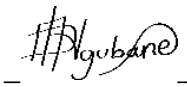
22 April 2021

Declaration

I declare that this dissertation is my own, unaided work. It is being submitted for the Degree of Master of Science at the University of the Witwatersrand, Johannesburg. It has not been submitted before for any degree or examination at any other University.

This project was carried out under the supervision of Dr. Yolandi Ernst (Global Change Institute) and the co-supervision of Prof. Francesca Parrini (School of Animal Plant and Environmental Science).

Signed: 22 April 2021 at The University of the Witwatersrand, Johannesburg



(Signature)

Abstract

Vegetation phenology is controlled by complex interactions between bottom up factors such as rainfall and top down factors such as fire and herbivory. Climate change has been shown to already be impacting the lowveld savanna landscape and is already causing long-term changes in vegetation. Phenology plays an important role in the carbon cycle; and therefore, understanding how long-term changes in phenology translate to changes in the carbon cycle is important. Our understanding of the long-term complex relationship between phenology and the carbon cycle is limited by a lack of continuous monitoring of phenology and carbon fluxes over large spatial extents. Therefore, the aim of my study was to utilize remote sensing data to analyse the long-term (18 years) phenology patterns at a landscape level in the savanna region and the relationship between vegetation phenology and the carbon cycle. I found that there was an advance in the end of season in the southern bioregion of the Kruger National Park albeit not due to changes in rainfall as expected. Moreover, I found concurrent changes in phenology) at a localized level indicating an interactive effect of top-down and bottom-up factors. In addition, I showed that there is a strong relationship between FAPAR (Fraction of Absorbed Photosynthetically Active Radiation) and Net Ecosystem Exchange (NEE). Moreover, there is a strong relationship between the start of season predicted using remote sensing and the start of carbon uptake derived from in-situ eddy covariance NEE. My results suggest that the long-term changes in phenology, especially the localized changes, may be driving long term changes in the carbon flux.

Key words: Phenology, Carbon cycle, Carbon Uptake, Bottom-up, Top-down

Acknowledgements

I would like to thank my supervisors Dr Yolandi Ernst and Prof. Francesca Parrini for their guidance, continuous support and for believing in me. Thank you for the opportunity you provided me to do my Master's degree with you, and for always reminding me of my potential and giving me confidence to always do better. I really appreciated your motivation along with the emotional support you always provided me.

Future Dr Hugo de Lemos, thank you for reminding me being curious about how things work is cool. I am grateful for the time you and Prof. Michele Verstraete took to assist me. This study would not be possible without the help of Miss Humbelani Thenga who provided the CSIR flux data.

I would also like to extend my thanks to the National Research Foundation, the Global Change Institute and the Carnegie Corporation of New York, for the funding they provided for this dissertation.

My mama. Thank you for the love and support. For affording me the chance to pursue my passion. To the boys coming after me, it's all possible. I believe in you; I hope you find the same belief within yourselves too.

Abbreviations and Symbols

ANOVA	-	Analysis of Variance
AVHRR	-	Advanced Very High-Resolution Radiometer
BRF	-	Bidirectional reflectance function
CFP	-	Carbon flux phenology
CSIR	-	Council for Scientific and Industrial Research
EC	-	Eddy covariance
EOS/ECU	-	End of season/End of carbon uptake
EVI	-	Enhanced vegetation index
FAPAR	-	Fraction of Absorbed Photosynthetically Active Radiation
JRC	-	Joint Research Centre
KNP	-	Kruger National Park
LAI	-	Leaf area index
LI	-	Large integral
LOS/CUP	-	Length of season/Carbon uptake period
LSP	-	Land surface phenology
MAR	-	Mean Annual Rainfall
MISR-HR	-	Multi-Angle Imaging SpectroRadiometer High Resolution
MODIS	-	Moderate Resolution Imaging Spectroradiometer
NDVI	-	Normalized Difference Vegetation Index
NEE	-	Net Ecosystem Exchange
POS/PCU	-	Peak of season/Peak of carbon uptake

RMSE	-	Root Mean Square Error
SOS/SCU	-	Start of season/Start of carbon uptake
STL	-	Seasonal trend decomposition by Leoss
%	-	Percent
˚C	-	Degrees Celsius

Dissertation structure

The first chapter provides a rationale, problem statement and a general introduction to the study as well as the literature review. The literature review gives context on the concept of phenology in the savanna landscape. Moreover, it provides context on previous methodologies used to conduct phenology studies in the savanna region.

The second chapter investigates the long-term change trends of vegetation phenology in different landscapes in the Kruger National Park. Here, I explore the differences in the phenology between the two main geologies of the KNP as well as the northern and southern bioregion. The third chapter investigates the relationship between remotely sensed phenology and in-situ derived phenology. It also assesses the performance of two FAPAR products from MODIS and MISR-HR.

In the last chapter I synthesize the key conclusions from the previous chapters and make suggestions for future studies.

Given that Chapters 2 and 3 have been prepared in publication format for submission to scientific journals, there is some degree of overlap with Chapter 1 and Chapter 4.

Contents

Declaration.....i

Abstract.....ii

Acknowledgements iii

Abbreviations and Symbols iv

Dissertation structure vi

List of Figures.....ix

List of Tables x

Chapter 1 1

1. Introduction.....1

1.1 Rationale.....1

1.2 Aim 4

1.3 Objectives 4

1.4. Literature Review 5

1.5. References 13

Chapter 2 20

2. Long-term changes in land surface phenology trends in the Kruger National Park over an 18-year period......20

2.1 Abstract.....20

2.2 Introduction 21

2.3 Methods 24

2.4 Results 27

2.6. References 39

Chapter 3 44

3. Matching land surface phenology with the phenology of net ecosystem exchange (NEE) in the Kruger National Park, South Africa. 44

3.1 Abstract.....44

3.2 Introduction 45

3.3 Methods 47
3.4 Results 51
.5 Discussion 55
3.6 References 59
Chapter 4 62
4. Discussion and Synthesis 62
4.1 References 66
5. Appendix 68

List of Figures

Figure 1.1 - A schematic of the MISR-HR Satellite instrument.

Figure 2.1 - The Kruger National Park (KNP) is located in the most north eastern part of South Africa occupying two provinces (Limpopo and Mpumalanga). The park is (a) divided into two main geology types (Basalt and Granite) and (b) has a north-south rainfall gradient roughly representative of a northern Mopane bioregion that receives lower mean annual rainfall (MAR) and a southern mixed woodland bioregion that receives a higher MAR (2001 – 2017). The woody cover map by Urban et al. (2020) in (c) shows differences between the two main geologies due to differences in nutrient availability (Venter and Gertenbach, 1986).

Figure 2.2 - Comparison of (a) mean start of season (SOS), (b) SOS variation, (c) mean length of season (LOS), (d) LOS variation, (e) mean end of season (EOS), (f) EOS variation, (g) mean large integral, (h) large integral variation, (i) mean annual rainfall as well as (j) mean rainfall variation between the basalt and granite geologies over an 18 year period (2001 – 2018) in the Kruger National Park.

Figure 2.3 - Comparison of (a) mean start of season, (b) start of season variation, (c) mean length of season, (d) length of season variation, (e) mean end of season, (f) end of season variation, (g) mean large integral, (h) large integral variation (i) mean annual rainfall, as well as the (j) mean rainfall variation between the north and south bioregions over an 18 year period (2001 – 2018) in the Kruger National Park.

Figure 2.4 - Pixel level raster regression of a) Start of season, b) End of season, c) Length of season and d) the large integral in the Kruger National Park for a period of 18 years (2001 – 2018). The green symbols indicate a significant increase whereby $R2 > 0.5$, $p < 0.05$ and slope >0, and the red symbols indicate a significant decrease whereby $R2 > 0.5$, $p < 0.05$ and slope <0.

Figure 3.1 - Illustrates the Kruger National Park (KNP) on the north-eastern part of South Africa. The Skukuza flux tower is located on the south-western part of the KNP in the granite geology.

Figure 3.2 - A comparison between a) MISR-HR and MODIS FAPAR, b) MISR-HR FAPAR and flux NEE and c) MODIS and flux NEE all fitted using the Savitzky Golay model at the Skukuza flux tower site, Kruger National Park.

Figure 3.3 - Cross-correlation between a) MISR-HR and NEE and b) MODIS and NEE. A single lag unit corresponds to 8-days for MODIS and 9/7 days for MISR-HR and corresponding NEE. The shaded bars show the highest correlation coefficient and the red horizontal represents the 95% confidence intervals.

Figure 3.4 - Figure 3.4: The relationship between the SOS of a) flux NEE and MISR-HR FAPAR and b) flux NEE and MODIS FAPAR in the Skukuza flux tower, Kruger National Park.

List of Tables

Table 2.1a - Percentage change within (1) granite geology, (2) basalt geology, (3) north region, and (4) the southern region over an 18-year period (2001 – 2018) in the Kruger National Park, South Africa.

Table 2.1b - Comparison of the percentage change in all the metrics across the park between the (1) granite geology, (2) basalt geology, (3) north region, and (4) the southern region over an 18-year period (2001 – 2018) in the Kruger National Park, South Africa.

Table 3.1 - Shows the abbreviations and notations used for the phenological metrics.

Table 3.2 - Relationships between carbon flux phenology and FAPAR phenology. NEE metrics ($SOS_{NEE,}$ EOS_{NEE}, CUP, and POS_{NEE}) were correlated to corresponding MISR and MODIS LSP metrics.

Table 3.3 - The differences in SOS, EOS, and POS between FAPAR derived from MODIS and MISR-HR and NEE (1 MODIS composite = 8 days; 1 MISR-HR composite 7/9 days)

Chapter 1

1. Introduction

1.1 Rationale

Savanna ecosystems cover a large spatial extent which represents one fifth of Earth's terrestrial ecosystems (Scholes and Hall, 1996). They are characterized by a continuous herbaceous layer interspersed with woody vegetation (Scholes and Walker, 1993). Through complex dynamic interactions between animals, plants, climatic factors and fire, savannas not only provide ecosystem services such as the provision of fuel wood, grazing and traditional medicinal plants but also play a large role in the carbon cycle (Scholes and Walker, 1993). Climate change is however expected to change these dynamics in the savanna system (Friedlingstein *et al.,* 2010; Van Wilgen et al., 2015).

Vegetation distribution and abundance in the Kruger National Park (KNP), South Africa, is driven by climatic variables such as temperature and precipitation in addition to biogeochemical factors such as soil type and nutrient availability (Scholes and Walker, 1993). Over the past six decades temperature has been increasing at a rate of 0.2 – 0.3 ˚C per decade while rainfall has shown increased interannual and seasonal variation over Southern Africa (Archer *et al.,* 2018). Changes in climate have been shown to alter seasonal vegetation development stages, therefore leading to either a decrease or an increase in vegetation photosynthetic activity which affects the carbon intake period and the Net Ecosystem Exchange (NEE) (Dragoni *et al.,* 2010; Keenan *et al.,* 2014; Buitenwerf et al., 2015).

Archibald and Scholes (2007) argued that phenology (timing of the specific growth and development stages in the annual or seasonal cycle) is well understood for temperate ecosystems, however, there is a lack of information on landscape phenology of South African savannas. The KNP, predominantly a savanna ecosystem, is one of the largest protected areas in South Africa (Eckhardt et al., 2000). The KNP is also considered an important carbon reservoir in South Africa with approximately 70 t/ha aboveground carbon (Yessoufou, 2017). Moreover, spanning across almost two million hectares, the KNP can potentially store an estimated 2×10^8 tonnes of above and belowground carbon (Yessoufou, 2017). However, it is important to note that the KNP as a carbon sink or a source is dependent on the seasonal photosynthetic activity of vegetation (Yessoufou, 2017).

As one of the largest emitters in Africa, South Africa is responsible for evaluating the contribution of the natural carbon sinks to offset carbon emissions as required by the Kyoto protocol (Shackleton and Scholes, 2011). Even though there have been studies that have analyzed the carbon stocks in the KNP, only a few have investigated the relationship between vegetation phenology patterns and the carbon cycle (Archibald *et al.*, 2009; Shackleton and Scholes, 2011; Yessoufou, 2017). Understanding phenology changes has important benefits because it allows for an understanding of how the carbon stock may change in response to climatic changes.

However, it is equally important to understand the vegetation phenology and changing trends thereof. The spatial heterogeneity in the savanna region makes it difficult to determine and define phenology due to temporal niche separation (Archibald and Scholes, 2007; Higgins et al., 2011). The temporal niche separation theory describes that many tree species, such as *Colophospermum mopane* (Mopane), have leaf-onset before the first rains of the season due to their ability to store water while grass and herbaceous species are limited by water availability (February and Higgins, 2016). This phenomenon creates complex spatio-temporal variability in vegetation seasonality in these landscapes resulting in different scales of responses to similar cues within the landscape due to heterogeneity (February and Higgins, 2016).

Quantification of vegetation phenological patterns in response to climate variables in the KNP has mostly been done using field data and continuous flux tower monitoring (Whitecross, 2016; Masia et al. 2018). Field observations only span a small spatial scale which does not represent the entire landscape (February et al., 2016). Remote sensing on the contrary provides frequent observations of the earth's surface area that cover a large spatial extent (Buitenwerf et al., 2015). Different studies have made use of vegetation indices in order to analyze phenological patterns in the lowveld region, however only a few have been done in the KNP (Archibald and Scholes, 2007; Parrini and Erasmus, 2009; Zurita-Mila, 2012; Ernst, 2018). Monitoring seasonal vegetation dynamics with vegetation indices (VIs) such as the Normalized Difference Vegetation Index (NDVI) is useful and often applied, however, they are not a direct biophysical measure of vegetation productivity.

The Fraction of Absorbed Photosynthetically Active Radiation (FAPAR) is a more direct measure of primary productivity and shows a positive and significant relationship with Gross Primary Productivity and Net Ecosystem Exchange (NEE) patterns (Archibald *et al.*, 2009;

Balzarolo *et al.*, 2015). It is well understood that when the growing season commences, the NEE unit becomes negative indicating the start of carbon sequestration (Verma *et al.*, 2014; Balzarolo *et al.*, 2015). Unlike vegetation indices that rely on vegetation greenness, FAPAR measures the actual photosynthetic activity, therefore, the use of FAPAR has the potential to present more ecologically accurate information on vegetation phenology and its relationship with carbon dynamics when compared to vegetation indices (Fensholt et al., 2004). Previous studies have also shown that NDVI is more sensitive to variations in leaf orientation, canopy structure, leaf properties, soil background and dead biomass on canopy than FAPAR (Myneni and Williams, 1994; Di Bella et al., 2004).

Several satellite earth observation products of FAPAR have been developed. Of these, MISR-HR FAPAR and MODIS fPAR [1](MODIS FAPAR[2]) have temporal coverage from 2000 until present, making them ideal for studying relatively long-term vegetation change trends. MISR-HR and MODIS sensors are both mounted on the Terra satellite platform and both use similar FAPAR retrieval models but acquire the Earth's surface data in different ways (Gobron and Verstraete, 2009). MISR-HR is a multi-angular sensor that considers vegetation anisotropy while MODIS is a single angle sensor. Multi-angular observations vastly improve accuracy as they take into account the multi-directional reflectance of an object caused by the object's geometry and illumination geometry (Pinty et al., 2007).

MISR-HR, however, is very sensitive to cloud contamination which results in the loss of a 17.6 km observation region per image due to the atmospheric correction approach that is utilized (Verstraete et al 2012). MODIS is also affected by cloud contamination; however, it uses a maximum value compositing approach (MVC) whereby the observation with the highest FAPAR value is selected out of the images over each 8-day composite period (Brown et al., 2020). The MVC approach improves the availability of data temporally but leads to overestimation of FAPAR by MODIS. Therefore, establishing which satellite sensor provides more consistent and ecologically accurate information is useful for future spatio-temporal studies of vegetation change and phenological patterns. An investigation of the relationship between FAPAR phenology from the two sensors and Net Ecosystem Exchange phenology will therefore provide an insight on how vegetation phenology patterns correlate to the carbon dynamics in the KNP.

[1] MODIS fPAR refers to the name of the MODIS FAPAR product.
[2] MODIS FAPAR refers to the product.

1.2 Aim

To gain an understanding of vegetation phenology trends across the KNP landscape using MODIS FAPAR and how phenology relates to carbon dynamics at the Skukuza fluxtower site using two remote sensing FAPAR products (MODIS and MISR-HR FAPAR) and Eddy Covariance NEE over an 18-year period.

1.3 Objectives

Objective 1

To quantify and describe phenological metrics and trends derived from MODIS FAPAR between two dominant geologies (basalt and granite) and bioregions (low rainfall northern region and higher rainfall southern region).

***Question*:** What are the comparative spatio-temporal phenological trends for the two geologies and two bioregions between 2001 and 2018 across the Kruger National Park with specific reference to the following phenological metrics?

a) Start of Season (SOS)

b) End of Season (EOS)

c) Length of Season (LOS)

d) FAPAR Large Integral (LI) – productivity metric used as proxy for accumulated biomass (Wessels et al., 2011)

Objective 2

To evaluate and compare the differences and similarities between phenological metrics derived from MISR-HR FAPAR, MODIS fPAR and in situ Net Ecosystem Exchange (NEE) with respect to the NEE phenology at the Skukuza flux tower sites over an 18-year period (2000 – 2018).

***Question 1*:** What is the correlation between FAPAR and NEE time series?

***Question 2*:** What is the relationship between land surface phenological metrics derived from MODIS and MISR-HR FAPAR and carbon flux phenology metrics derived from Net Ecosystem Exchange?

1.4. Literature Review

1.4.1 The South African Savanna

The co-dominance of different trees and grasses, coupled with strong seasonality, distinguishes the savanna from other biomes (Scholes and Archer, 1997). The relative abundance, and spatial distribution of woody vegetation and grasses in the savanna are controlled by complex dynamic interactions between fire, herbivory, climate, soils,water, nutrients and geomorphology resulting in high spatial heterogeneity (Scholes and Archer, 1997). Savannas contribute a substantial amount to global terrestrial primary productivity and are only second after tropical forests (Scholes and Walker, 1993).

The South African savanna biome is essential to conservation of biodiversity and tourism, and therefore contributes hundreds of millions of dollars as it is home to diverse endemic and indigenous flora and fauna (Scholes and Walker, 1993). The KNP is surrounded by peri-urban development and villages, especially on its southern and western boundaries (SANParks, 2017). With the high unemployment rate in the Limpopo province (38.2% in 2017), the KNP is considered to be one of the most important sources of economic resources (R850 million during the 2016/17 financial year) for the surrounding communities as most of the park employees are from the surrounding local communities (Swemmer et al., 2017; Chikadel and Child, 2020). Besides the high socio-economic value, KNP has about 2000 plant species of which around 400 are tree species and 220 are grass species (SANParks, 2017). The Kruger National Park is also home to around 150 mammals, 120 reptile, 50 fish, 500 bird and 30 amphibian species.

Therefore, the park represents a complex and dynamic system with important interactions between vegetation and fauna. With climate change, changes to vegetation distribution is likely to have an impact, not only on the vegetation species diversity, but also the fauna diversity and all associated ecosystem services (SANParks, 2017; Dube and Nhamo, 2020).

1.4.2 Plant phenology

Phenology is the scientific study of the timing of recurring biological events or cycles (Schaber *et al.,* 2010). It is considered to be an integrated science that also comprises the study of the interactions between biotic and abiotic factors that cause the specific timing of these events (Schaber *et al.,* 2010; Elmendorf *et al.,* 2016). The timing of specific growth and development stages in the annual or seasonal cycle is driven mainly by climatic shifts as well as localized variation in soil type (Richardson and O'keef, 2009). Plant species are well adapted to their niches and make up distinct ecosystems based on their adaptations to their environments (Richardson and O'Keef, 2009). Changes in these environments due to human activities and climate change usually lead to various responses from different plant functional types (Richardson and O'Keef, 2009). These may include but are not limited to changes in distribution, physiological adjustments such as changes in respiration rates, carbon uptake periods and photosynthetic capacity among others (Crous, 2019). Over time, different plant species have evolved adaptability traits that allow them to utilize environmental cues indicating resource availability and season. At the individual plant level, response types include changes in the timing of life cycle events such as leaf unfolding, bud-burst and leaf fall, amongst others (van Vliet, 2010). Two biotic oscillations (diurnal and seasonal) drive these plant life cycles through plant primary productivity and/or plant community photosynthesis (Gu *et al.,* 2009).

The diurnal cycle is well understood in terms of its effect on various plant functional types. It controls light energy available for photochemical processes as well as relative water content, ambient air temperature and relative humidity and therefore is fairly predictable (Popescu and Popescu, 2014). The seasonal cycle, however, is driven by various interdependent factors such as moisture, nutrient availability, photoperiod and radiation, with climatic factors such as precipitation and temperature likely playing the most important role (Popescu and Popescu, 2014). These factors have been shown to be the primary drivers of canopy greenness and affect phenology of different plants in different ways (Garonna, 2016). Seasonal cycles are expected to shift as climatic variables change in the future and there is limited knowledge on how savanna ecosystems are going to respond.

1.4.3 Evidence and impacts of phenology shifts

In South Africa the last three decades have been warmer than any other preceding decade since the 1800s, with 2017 reported as the hottest year on record while inter-annual variation of precipitation has increased (Archer *et al.,* 2018). Changes in these climate variables affect seasonality and may cause either a delay or an advance of the timing of life cycle events of different species (Schaber *et al.,* 2010). Phenological patterns are therefore regarded as some of the most apparent and obvious documented evidence of the impact of climate warming (Forrest and Miller-Rushing, 2010). Even though climatic variables drive phenology; phenology plays a role on global climate through its control on carbon intake and assimilation (Chuine, 2010; Irving, 2015). Later timing of leaf senescence and earlier leaf unfolding associated with climate warming result in longer carbon assimilation and uptake as well as higher net primary productivity (Jolly and Steven, 2004; Chuine, 2010).

Climate warming has different impacts on carbon uptake in different seasons. At the beginning of the wet season warmer temperatures enhance growth more than soil decomposition while this is the opposite in the dry season (Chuine, 2010). Data from CO_2 flux towers across the temperate latitudes and dynamic global vegetation models show that early dry season warming has more influence on the net ecosystem exchange compared to early wet season warming (Chuine, 2010). In this case, the landscape acts as a carbon source when autumn warming occurs despite early leaf unfolding (Chuine, 2010). In the South African savanna, the dry and wet season show the highest net primary productivity at a savanna flux site when leaves are present (Archibald *et al.,* 2009). Therefore, the length of green leaf retention during both seasons in this savanna system is important to understanding NEE (Higgins et al., 2011; February and Higgins, 2016; February et al., 2020).

Net ecosystem exchange seasonality is often described as carbon flux phenology as it represents seasonal gross photosynthesis (Verma *et al.,* 2014; Balzarolo *et al.,* 2016). For instance, studies in a number of biomes including deciduous forests, woody savannas and grasslands show that there is a strong link between phenology and the dynamic nature of carbon stocks in an ecosystem (Zhu et al., 2013; Balzarolo et al., 2016). For the Kruger National Park, however, only the study by Archibald et al. 2009 has described the association between vegetation seasonality and carbon flux phenology in the savanna region. Additionally, the research only focused on vegetation greenness in relation to NEE over a short temporal extent and therefore could not show how the leaf greenness has changed over

time. There is therefore a need to understand the specific relationship between vegetation seasonality and carbon flux phenology within the KNP savanna landscape.

1.4.4 Deriving phenology parameters

Seasonal leaf display patterns are usually associated with primary productivity, and thus deriving phenology metrics from these patterns reduces subjective interpretation that is common in visual estimation of phenology (Fitchett and Grab, 2015). Length of the dormant season, length of the growing season, green-up date, length of the green-up period, date of first leaf drop, and length of the dry down period are examples of visual phenological metrics that have been recently used in the savanna (Masia *et al.,* 2018). Similar metrics can be derived statistically from vegetation indices and these include start of season (SOS), length of season (LOS) and the end of season (EOS). Additional methods that are used to derive phenology metrics include digital repeat photography, phenology models and experiments (Fitchett and Grab, 2015). An example of vegetation indices and modelling is a study by Archibald and Scholes (2007) which developed a phenology model using the Advanced Very High-Resolution Radiometer (AVHRR) in the South African savanna and found that the model could predict 86% of the onset of plant green-up.

In-situ Phenological observations

Ground-based phenological observations are regarded as the most predominant phenology methodology that spans back to 1300 AD in historical data (Ledneva *et al.,* 2004). However, repeatable, scalable and comparable phenological studies increased only in the 1990s as a way to provide some answers about the impacts of climate change (Menzel *et al.,* 2006). Ground-based observations entail visual monitoring of vegetation species at different temporal and spatial scales (Fitchett and Grab, 2015). Visual monitoring is usually done by multiple individuals in order to cover a larger spatial extent or to increase the frequency of observations. Even though phenological events such as flowering, bud-burst, leaf unfolding, and coloration are well described for certain species, there are a few limitations associated with this method (Fitchett and Grab, 2015).

Describing the phenological events remains subjective as it depends on personal interpretation of these events and the consistency of data collection is affected by the level of commitment. When there are more observers, the inconsistency of the data increases even more. Climate and accessibility of the specific species of interest or plant functional type also

plays a role on the consistency or the quality of the dataset (Fitchett and Grab, 2015). To account for the aforementioned inconsistency, commercially available hand-held devices, and field spectroradiometers are used. However, field observations are limited to a small spatial extent and therefore remain labor intensive and expensive for continuous monitoring. In recent years, there has been an adoption of remote sensing techniques to study plant phenology due to advances in technology. Remote sensing techniques aim to address some of the limitations of ground-based observations such as spatio-temporal coverage and consistency of data. However, in-situ observations are as important as they are often used to validate satellite derived phenology.

Remote sensing of phenology – Land Surface Phenology (LSP)

Plant phenology analyzed at a landscape or global scale through space-borne earth observation or remote sensing is referred to as Land Surface Phenology (LSP) (Gessner *et al.*, 2015). Thus far, most land surface phenology models have been based on vegetation indices such as the enhanced vegetation index (EVI) and the normalized difference vegetation index (NDVI) (Cho *et al.*, 2017). These two indices are not physical properties or parameters for vegetation, rather, they are proxies for canopy greenness.

In open savanna landscapes, NDVI is a good indicator of leaf area since it usually does not reach its saturation levels (Scholes and Archibald, 2007). The NDVI is based on the premise that healthy vegetation absorbs blue and red spectral bands and reflects the green spectral band in the electromagnetic spectrum. The near and shortwave infrared parts of the spectrum have high reflectance on vegetation due to cell structure. The NDVI is calculated using the red (R) spectral bands as they show the strongest absorption and the near infrared (NIR) band as it shows the weakest absorption.

$$NDVI = \frac{NIR - R}{NIR + R}$$

Despite its wide usage in vegetation analysis and land surface phenology, NDVI has a few limitations. Since NDVI is calculated using the absorption and reflectance bands of vegetation, its value for two vegetation types with similar biophysical properties can differ vastly depending on how much soil background is exposed (Huete *et al.*, 1985; Yengoh *et al.*, 2015). This limitation is particularly important especially in the savanna region where vegetation may be fragmented depending on land use form (Scholes and Walker, 1993). The savanna region is a heterogeneous landscape with clumps and patches of vegetation

sometimes on bare soil (Scholes and Walker, 1993). NDVI is also highly sensitive to atmospheric absorption and scattering of radiation since it utilizes the red band that has short wavelengths. It also reaches a saturation level when analyzing vegetation with high leaf area index (LAI) and it cannot differentiate the greenness of the vegetation (Gitelson, 2004; Scholes and Archibald, 2007). The LAI and FAPAR are useful alternatives to vegetation indices as they are biophysical properties or parameters for photosynthetic productivity.

FAPAR is the ratio of the photosynthetic photon flux density which is measured above or below the canopy on the visible section of the electromagnetic spectrum (Li *et al.,* 2015). It is a measure of the radiation that is absorbed by plants during photosynthetic processes and considers the radiation that is reflected from the understory and/or from the canopy (Li *et al.,* 2015). There are different types of FAPAR observations when utilizing remote sensing techniques. Outgoing and incoming photosynthetically active radiation (PAR) either horizontally or vertically constitute the total FAPAR (Gobron and Verstraete, 2009). Incoming FAPAR is partitioned into two categories, 1) at the top of canopy which is referred to as direct or diffuse and 2) horizontally propagating PAR (Gobron and Verstraete, 2009). Outgoing FAPAR includes PAR reflected by the top and the bottom of the canopy (Gobron and Verstraete, 2009). The total FAPAR also takes into account the light that is reflected by bare soil or the understory (Weiss and Baret, 2010).

There are several remote sensing satellite sensors that retrieve FAPAR using different retrieval methods such as inversion methods, neural networks, optimization based on radiative transfer models and parametric relation with the LAI (Gobron and Verstraete, 2009). These satellite products include the ESA-MERIS-FAPAR, MODIS LAI/fPAR, MISR-HR LAI/FAPAR, and LANDSAF. Most of these satellite instruments have a single optical sensor that retrieves data at nadir (the position directly below the satellite) (Gobron and Verstraete, 2009). The MODIS and MISR-HR sensors both use the bidirectional reflectance function (BRF) which characterizes the angular signature of canopy reflectance (Knyazikhin *et al.,* 1998). MISR-HR and MODIS are hosted on the same satellite platform and both utilize 3D inversion models based on a look up table with different land cover types to retrieve FAPAR/fPAR (Gobron and Verstraete, 2009). The single angle MODIS uses seven spectral bands and a land cover product for retrieval of vegetation biophysical parameters such as LAI and FAPAR while MISR-HR[3] uses four spectral bands (Knyazikhin *et al.,* 1998). Vegetation

[3] Multi-Angle imaging SpectroRadiometer High Resolution (275 m)

as a 3D structure is anisotropic, meaning it has different reflectance values when measured at different angles (Verstraete *et al.,* 2012). The fundamental difference between MODIS fPAR and MISR-HR FAPAR is the number of angles at which surface information is recorded (Gobron and Verstraete, 2009). The multi-angular MISR-HR takes into account the different reflectance values which enables better retrieval of land surface products that are less affected by shadows (Pinty *et al.,* 2007). Pinty *et al. (*2007) show that the difference between MISR-HR FAPAR and MODIS fPAR reaches up to 0.23 (on a scale of 0 – 1). MODIS fPAR product also tends to have an analogous bias towards high FAPAR values (Pinty *et al.,* 2007).

The Multi-angle Imaging Spectroradiometer (MISR[4]) was built by the Jet Propulsion Laboratory and is hosted on the NASA Terra platform. The platform has a 16 day repeat cycle around the equator and follows 233 orbital paths (Verstraete *et al.,* 2012). MISR has been operational since the year 2000 and that allows for an analysis of long-term environmental change. It takes advantage of its nine different sensors which capture the surface of the Earth all at the same time. The MISR satellite therefore reduces the impact that anisotropy has on reflectance values of an object on the surface through four front off-nadir sensors, a nadir sensor and another four rear off-nadir sensors (Verstraete *et al.,* 2012).

MISR collects data in the visible part of the electromagnetic spectrum and the near infrared region from the sunlit side of the planet Earth (Verstraete *et al.,* 2012). In total, 36 data observations are acquired though the 9 sensors for the four spectral bands (Figure 1.1). The data is collected on two different modes which have different spatial resolutions. The global mode acquires data at 1.1 km resolution with negligible information loss that is retrievable through the Joint Research Center (JRC) sharpening method (Verstraete *et al.,* 2012). To increase instrumental data rate, non-red spectral bands of the off-nadir sensors are spatially averaged using 4 x 4 pixels in global mode. However, three data channels are kept at native resolution of 275 m. These channels are 1) the spectral bands of the nadir camera, 2) the red spectral band of the off-nadir camera and 3) the red spectral band of the nadir camera. This makes a total of 16 data channels at native resolution in global mode. The local mode acquires surface information at 275 m resolution and is referred to as MISR High Resolution (MISR-HR). MISR has several final products but the most important in this study is FAPAR which is acquired through a series of integration and inversion processes (Verstraete *et al.,* 2012).

[4] Multi-Angle imaging SpectroRadiometer (1.1 km)

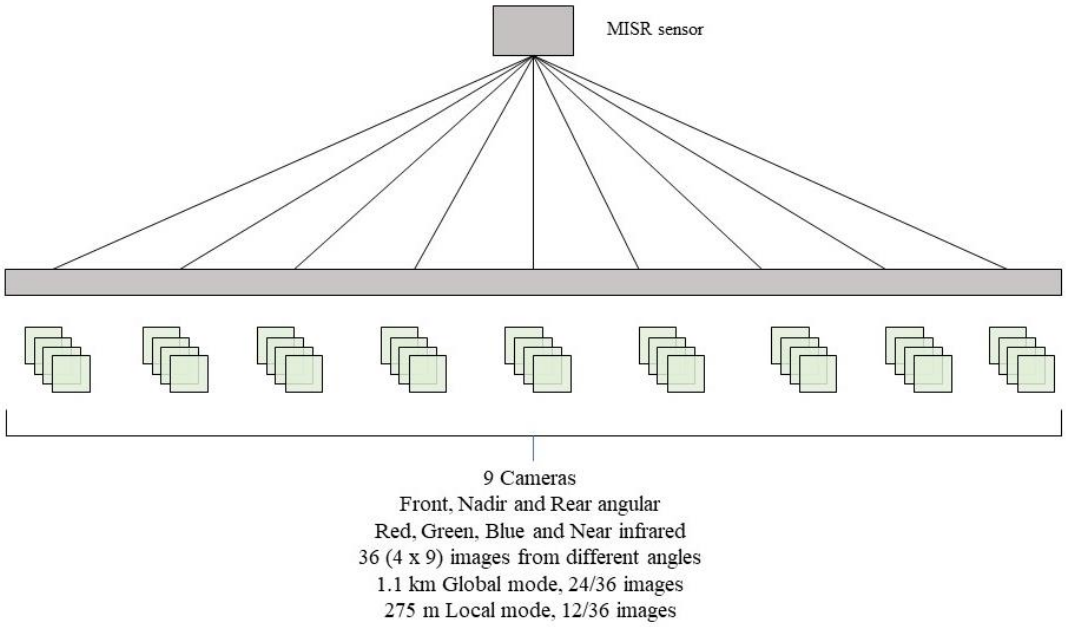


Figure 1.1: A schematic of the MISR Satellite instrument.

1.5. References

Archer, E.R., Engelbrecht, F.A., Hänsler, A., Landman, W., Tadross, M. and Helmschrot, J., 2018. Seasonal prediction and regional climate projections for southern Africa. In *Climate change and adaptive land management in southern Africa – assessments, changes, challenges, and solutions,* pp. 14-21 Klaus Hess Publishers.

Archibald, S. A., Kirton, A., van der Merwe, M. R., Scholes, R. J., Williams, C. A., and Hanan, N. 2009. Drivers of inter-annual variability in net ecosystem exchange in a semi-arid savanna ecosystem, South Africa. *Biogeosciences*, 6, pp. 251–266.

Archibald, S. and Scholes, R.J., 2007. Leaf green-up in a semi-arid African savanna-separating tree and grass responses to environmental cues. *Journal of Vegetation Science*, *18*(4), pp.583-594.

Balzarolo, M., Vicca, S., Nguy-Robertson, A.L., Bonal, D., Elbers, J.A., Fu, Y.H., Grünwald, T., Horemans, J.A., Papale, D., Peñuelas, J. and Suyker, A., 2016. Matching the phenology of net ecosystem exchange and vegetation indices estimated with MODIS and FLUXNET in-situ observations. *Remote Sensing of Environment*, *174*, pp.290-300.

Buitenwerf, R., Rose, L. and Higgins, S.I., 2015. Three decades of multi-dimensional change in global leaf phenology. *Nature Climate Change*, *5*(4), pp.364-368.

Chidakel, A., Eb, C. and Child, B., 2020. The comparative financial and economic performance of protected areas in the Greater Kruger National Park, South Africa: Functional diversity and resilience in the socio-economics of a landscape-scale reserve network. *Journal of Sustainable Tourism*, *28*(8), pp.1100-1119.

Cho, M.A., Ramoelo, A. and Dziba, L., 2017. Response of land surface phenology to variation in tree cover during green-up and senescence periods in the semi-arid savanna of Southern Africa. *Remote Sensing*, *9*(7), p.689.

Chuine, I., 2010. Why does phenology drive species distribution? *Philosophical Transactions of The Royal Society: Biological Sciences*, 365, pp. 3149-3160.

Crous, K.Y., 2019. Plant responses to climate warming: physiological adjustments and implications for plant functioning in a future, warmer world. *American journal of botany*, *106*(8), p.1049.

Di Bella, C.M., Paruelo, J.M., Becerra, J.E., Bacour, C. and Baret, F., 2004. Effect of senescent leaves on NDVI-based estimates of f APAR: Experimental and modelling evidences. *International Journal of Remote Sensing*, *25*(23), pp.5415-5427.

Dragoni, D., Schmid, H.P., Wayson, C.A., Potter, H., Grimmond, C.S.B. and Randolph, J.C., 2011. Evidence of increased net ecosystem productivity associated with a longer vegetated season in a deciduous forest in south-central Indiana, USA. *Global Change Biology*, *17*(2), pp.886-897.

Dube, K. and Nhamo, G., 2020. Evidence and impact of climate change on South African national parks. Potential implications for tourism in the Kruger National Park. *Environmental Development*, *33*, p.100485.

Du Toit, J.T., Rogers, K.H. and Biggs, H.C., 2003. Vegetation dynamics in the Kruger ecosystem, In *The Kruger experience: ecology and management of savanna heterogeneity*, Island Press. *Washington, DC, US*.

Eckhardt, H., Van Wilgen, B.W. and Biggs, H., 2000, 'Trends in woody vegetation cover in the Kruger National Park, South Africa, between 1940 and 1998', *African Journal of Ecology* 38(2), pp.108–115.

Elmendorf, S.C., Jones, K.D., Cook, B.I., Diez, J.M., Enquist, C.A., Hufft, R.A., Jones, M.O., Mazer, S.J., Miller-Rushing, A.J., Moore, D.J. and Schwartz, M.D., 2016. The plant phenology monitoring design for the National Ecological Observatory Network. *Ecosphere*, *7*(4), p.e01303.

Ernst, Y.M., 2018. *Spatio-temporal trends in vegetation dynamics across a savanna-dominated national park* (Doctoral dissertation).

February, E.C. and Higgins, S.I., 2016. Rapid leaf deployment strategies in a deciduous savanna. *PloS one*, *11*(6), p.e0157833.

February, E., Pausch, J. and Higgins, S.I., 2020. Major contribution of grass roots to soil carbon pools and CO 2 fluxes in a mesic savanna. *Plant and Soil*, *454*(1), pp.207-215.

Fitchett, J.M., Grab, S.W. and Thompson, D.I., 2015. Plant Phenology and Climate Change: Progress in Methodological Approaches and Applications. *Progress in Physical Geography*, 39, pp. 460-482.

Garonna, I., De Jong, R. and Schaepman, M.E., 2016. Variability and evolution of global land surface phenology over the past three decades (1982–2012). *Global change biology*, *22*(4), pp.1456-1468.

Gitelson, A.A., 2004. Wide dynamic range vegetation index for remote quantification of biophysical characteristics of vegetation. *Journal of plant physiology*, *161*(2), pp.165-173.

Gobron, N. and Verstraete, M., 2009. ECV T10: Fraction of Absorbed Photosynthetically Active Radiation (FAPAR). *Essential Climate Variables*, p.23.

Gu, L., Post, W.M., Baldocchi, D.D., Black, T.A., Suyker, A.E., Verma, S.B., Vesala, T. and Wofsy, S.C., 2009. Characterizing the seasonal dynamics of plant community photosynthesis across a range of vegetation types. In *Phenology of ecosystem processes* (pp.35-58). Springer, New York, NY.

Hu, J., Su, Y., Tan, B., Huang, D., Yang, W., Schull, M., Bull, M.A., Martonchik, J.V., Diner, D.J., Knyazikhin, Y. and Myneni, R.B., 2007. Analysis of the MISR LAI/FPAR product for spatial and temporal coverage, accuracy and consistency. *Remote Sensing of Environment*, *107*(1-2), pp.334-347.

Higgins, S.I., Delgado-Cartay, M.D., February, E.C. and Combrink, H.J., 2011. Is there a temporal niche separation in the leaf phenology of savanna trees and grasses?. *Journal of Biogeography*, *38*(11), pp.2165-2175.

Irving LJ. 2015. Carbon assimilation, biomass partitioning and productivity in grasses. *Agriculture*. 5(4), pp.1116–1134.

Jin, C., Xiao, X., Merbold, L., Arneth, A., Veenendaal, E. and Kutsch, W.L., 2013. Phenology and gross primary production of two dominant savanna woodland ecosystems in Southern Africa. *Remote Sensing of Environment*, 135, pp.189-201.

Jolly, W. M., and Running, S. W. (2004). Effects of precipitation and soil water potential on drought deciduous phenology in the Kalahari. *Global Change Biology*, 10, pp.303–308.

Jones, L.A., Kimball, J.S., Reichle, R.H., Madani, N., Glassy, J., Ardizzone, J.V., Colliander, A., Cleverly, J., Desai, A.R., Eamus, D. and Euskirchen, E.S., 2017. The SMAP Level 4 Carbon Product for Monitoring Ecosystem Land–Atmosphere CO 2

Exchange. *IEEE Transactions on Geoscience and Remote Sensing*, *55*(11), pp.6517-6532.

Keenan, T.F., Gray, J., Friedl, M.A., Toomey, M., Bohrer, G., Hollinger, D.Y., Munger, J.W., O'Keefe, J., Schmid, H.P., Wing, I.S. and Yang, B., 2014. Net carbon uptake has increased through warming-induced changes in temperate forest phenology. *Nature Climate Change*, *4*(7), pp.598-604.

Knyazikhin, Y., Martonchik, J.V., Diner, D.J., Myneni, R.B., Verstraete, M., Pinty, B. and Gobron, N., 1998. Estimation of vegetation canopy leaf area index and fraction of absorbed photosynthetically active radiation from atmosphere-corrected MISR data. *Journal of Geophysical Research: Atmospheres*, *103*(D24), pp.32239-32256.

Knyazikhin, Y., Martonchik, J.V., Myneni, R.B., Diner, D.J. and Running, S.W., 1998. Synergistic algorithm for estimating vegetation canopy leaf area index and fraction of absorbed photosynthetically active radiation from MODIS and MISR data. *Journal of Geophysical Research: Atmospheres*, *103*(D24), pp.32257-32275.

Ledneva, A., Miller-Rushing, A.J., Primack, R.B. and Imbres, C., 2004. Climate change as reflected in a naturalist's diary, Middleborough, Massachusetts. *The Wilson Journal of Ornithology*, *116*(3), pp.224-232.

Li, W., Weiss, M., Waldner, F., Defourny, P., Demarez, V., Morin, D., Hagolle, O. and Baret, F., 2015. A generic algorithm to estimate LAI, FAPAR and FCOVER variables from SPOT4_HRVIR and landsat sensors: evaluation of the consistency and comparison with ground measurements. *Remote Sensing*, *7*(11), pp.15494-15516.

Ma, X., Huete, A., Yu, Q., Coupe, N.R., Davies, K., Broich, M., Ratana, P., Beringer, J., Hutley, L.B., Cleverly, J. and Boulain, N., 2013. Spatial patterns and temporal dynamics in savanna vegetation phenology across the North Australian Tropical Transect. *Remote sensing of Environment*, *139*, pp.97-115.

Makhado, R.A., Potgieter, M.J. and Luus-Powell, W.J., 2018. Colophospermum Mopane Leaf Production and Phe-nology in Southern Africa's Savanna Ecosystem-A Review. *Insights For Res*, *2*(1), pp.84-90.

Masia, N.D., Stevens, N. and Archibald, S., 2018. Identifying phenological functional types in savanna trees. *African Journal of Range and Forage Science*, *35*(2), pp.81-88.

Menzel, A., Sparks, T.H., Estrella, N., Koch, E., Aasa, A., Ahas, R., Alm-Kübler, K., Bissolli, P., Braslavská, O.G., Briede, A. and Chmielewski, F.M., 2006. European phenological response to climate change matches the warming pattern. *Global change biology*, *12*(10), pp.1969-1976.

Myneni, R.B. and Williams, D.L., 1994. On the relationship between FAPAR and NDVI. *Remote Sensing of Environment*, *49*(3), pp.200-211.

Parrini, F. and Erasmus, B.F.N., 2009. Spatial and temporal heterogeneity of phenology patterns in Kruger National Park, South Africa: different drivers for different areas. In *Proceedings, 33rd International Symposium on Remote Sensing of Environment, ISRSE* (Vol. 2009, pp.627-631).

Pinty, B., Lavergne, T., Voßbeck, M., Kaminski, T., Aussedat, O., Giering, R., Gobron, N., Taberner, M., Verstraete, M.M. and Widlowski, J.L., 2007. Retrieving surface parameters for climate models from Moderate Resolution Imaging Spectroradiometer (MODIS)-Multiangle Imaging Spectroradiometer (MISR) albedo products. *Journal of Geophysical Research: Atmospheres*, *112*(D10).

Popescu, M. and Popescu, G.C., 2014. Diurnal changes in leaf photosynthesis and relative water content of grapevine. *Current Trends in Natural Sciences Vol*, *3*(6), pp.74-81.

Richardson, A.D. and O'Keefe, J., 2009. Phenological differences between understory and overstory. In *Phenology of ecosystem processes* (pp.87-117). Springer, New York, NY.

Schaber, J., Badeck, F., Doktor, D. and von Bloh, W., 2010. Combining messy phenological time series. *In Phenological Research* (pp.147-158). Springer, Dordrecht.

Scholes, R. J., and Archer, S. R. (1997). Tree-grass interactions in savannas. *Annual Review of Ecology and Systematics*, 28, pp.517–544.

Scholes, R. J., and Hall, D. O. (1996). *The carbon budget of tropical savannas, woodlands and grasslands.* New York: John Wiley and Sons.

Scholes, R.J. and Walker, B.H. 1993. *An African savanna: a synthesis of the Nylsvlei study.* Cambridge University Press, Cambridge, UK.

Shackleton, C.M. and Scholes, R.J., 2011. Above ground woody community attributes, biomass and carbon stocks along a rainfall gradient in the savannas of the central lowveld, South Africa. *South African Journal of Botany*, *77*(1), pp.184-192.

Simioni, G., Gignoux, J., Le Roux, X., Appé, R., Benest, D., 2004. Spatial and temporal variations in leaf area index, specific leaf area and leaf nitrogen of two co-occurring savanna tree species. *Tree Physiology*, 24, pp.205–216.

South African National Parks (SANParks). 2017. *Kruger National Park Management Plan 2018 – 2028*, Pretoria, South Africa. [Online] URL: https://www.sanparks.org/assets/docs/conservation/park_man/knp/draft-plan.pdf

Swemmer, L., Mmethi, H. and Twine, W., 2017. Tracing the cost/benefit pathway of protected areas: A case study of the Kruger National Park, South Africa. Ecosystem services, 28, pp.162-172.

van Vliet, A.J., 2010. Societal adaptation options to changes in phenology. In *Phenological Research* (pp. 75-98). Springer, Dordrecht.

van Wilgen, N.J., Goodall, V., Holness, S., Chown, S.L. and McGeoch, M.A., 2016. Rising temperatures and changing rainfall patterns in South Africa's national parks. *International Journal of Climatology*, *36*(2), pp.706-721.

Verma, M., Friedl, M.A., Richardson, A.D., Kiely, G., Cescatti, A., Law, B.E., Wohlfahrt, G., Gielen, B., Roupsard, O., Moors, E.J. and Toscano, P., 2014. Remote sensing of annual terrestrial gross primary productivity from MODIS: an assessment using the FLUXNET La Thuile data set. *Biogeosciences*, *11*(8), p.2185.

Weiss, M. and Baret, F., 2011. *fAPAR (fraction of Absorbed Photosynthetically Active Radiation) estimates at various scale.* In Proceedings of the 34th International Symposium for Remote Sensing of the Environment (ISRSE), Sydney, Australia (pp. 10-15).

Wessels, K., Steenkamp, K., Von Maltitz, G. and Archibald, S., 2011. Remotely sensed vegetation phenology for describing and predicting the biomes of South Africa. *Applied Vegetation Science*, *14*(1), pp.49-66.

Whitecross, M.A., Witkowski, E.T.F. and Archibald, S., 2017. Savanna tree-grass interactions: A phenological investigation of green-up in relation to water availability over three seasons. *South African Journal of Botany*, *108*, pp.29-40.

Yengoh, G.T., Dent, D., Olsson, L., Tengberg, A.E. and Tucker, C.J., 2015. Limits to the Use of NDVI in Land Degradation Assessment. In *Use of the Normalized Difference Vegetation Index (NDVI) to Assess Land Degradation at Multiple Scales* (pp.27-30). Springer, Cham.

Yessoufou, K., 2017. Potential carbon stock in the Kruger National Park, South Africa. *Botany Letters*, *164*(4), pp.425-432.

Zhu, W., Chen, G., Jiang, N., Liu, J. and Mou, M., 2013. Estimating carbon flux phenology with satellite-derived land surface phenology and climate drivers for different biomes: A synthesis of AmeriFlux observations. *PloS one*, *8*(12), p.e84990.

Zurita-Milla, R., Van Gijsel, J.A.E., Hamm, N.A., Augustijn, P.W.M. and Vrieling, A., 2012. Exploring spatiotemporal phenological patterns and trajectories using self-organizing maps. *IEEE Transactions on geoscience and remote sensing*, *51*(4), pp.1914-1921.

Chapter 2

2. Long-term changes in land surface phenology trends in the Kruger National Park over an 18-year period.

2.1 Abstract

The Kruger National Park, a protected area within the savanna biome, is an excellent landscape for studying the seasonality of savanna vegetation phenology due to its broad scale differences in vegetation types owing to contrasting underlying geologies and a rainfall gradient. Moreover, very little is known about the long-term phenology trends and the role that changing climate, especially rainfall, might be playing in this landscape. I, therefore, aimed to describe and compare the spatio-temporal phenological patterns and trends between the basalt and granite geologies and between the relatively lower rainfall northern region and the relatively higher rainfall southern region between 2001 and 2018. I found no relationship between the change trends of precipitation and the vegetation seasonality in the park. My findings indicated that the end of season advanced by a week to a week and a half in the southern bioregion of the park. Additionally, there were significant and concurrent localized change trends in all the metrics used in this study, likely resulting from an interactive effect of soil moisture, fire, and herbivory. The localized decreases in Length of Season (LOS) and Large integral (LI) suggest that there was shortening of length of season as well as a decrease in the amount of accumulated biomass across the park. Due to the semi-arid nature of the park, the general phenology of varied vegetation functional types is mainly influenced by climate, and soil moisture. However top down factors such as fire and herbivory were most likely the cause of the observed phenological change trends. Continued monitoring of phenology trends and drivers is essential for understanding the anticipated consequences of a changing climate. This study provides insight on how vegetation phenology has changed in the savanna region within the Kruger National Park over the past two decades.

Keywords: Phenology, Carbon cycle, Global change, Seasonality, Bioregions, Geology

2.2 Introduction

Characterized by the co-existence of a continuous herbaceous layer interspersed with woody vegetation, savanna ecosystems represent one of the most complex and dynamic landscapes (Scholes and Walker, 1993). The semi-arid nature of southern African savannas makes precipitation/water availability a crucial and often a limiting factor for vegetation productivity (Archibald and Scholes, 2007).

Climate change is however already changing these dynamics in the savanna system (MacFadyen et al., 2016; Van Wilgen et al., 2016; Dube and Nhamo, 2019). Over the past six decades temperature has been increasing at a rate of 0.2 – 0.3 ˚C per decade while rainfall variability increased within and between seasons across southern Africa (Archer *et al.,* 2018). Changes in rainfall especially have been shown to alter seasonal vegetation development stages, therefore leading to either a decrease or an increase in vegetation photosynthetic activity which affects the carbon intake period and the Net Ecosystem Exchange (NEE) (Dragoni *et al.,* 2010; Keenan *et al.,* 2014).

Phenology (timing of the specific growth and development stages in the annual or seasonal cycle) is well understood for temperate ecosystems, however, there is a lack of information on landscape phenology of South African savannas (Chudimayo, 2001; Archibald and Scholes 2007; Higgins et al., 2011; Jin et al., 2013; Whitecross et al., 2017). This finding remains relevant to date. Unlike in the northern hemisphere and in temperate systems where temperature and photoperiod dominantly determine the growth of vegetation functional types (Archibald and Scholes, 2007), vegetation growth and seasonality in African savannas is driven to a large extent by rainfall (Chudimayo , 2001; Higgins et al., 2011) and the plant-types' ability to store water and nutrients (Archibald and Scholes, 2007; February et al., 2016). Therefore, the vegetation seasonal responses to changes in precipitation at the landscape scale are essentially dependent on vegetation structure and function (Higgins et al., 2011). The temporal niche separation theory describes that many tree species, such as *Colophospermum Mopane* (Mopane), have leaf-onset before the first rains of the season due to their ability to store water and nutrients while grasses and forbes are limited by water availability (Simioni et al., 2004; Scholes and Archibald, 2007 and Makhado et al., 2018). This heterogeneity creates complex spatio-temporal variability in vegetation seasonality in these landscapes resulting in different scales of responses to similar drivers of change within the landscape (Higgins et al., 2007).

The Kruger National Park, in South Africa, which is a protected area within the Savanna biome, presents a unique landscape for studying savanna vegetation seasonality. Firstly, vegetation distribution and abundance are driven by climatic variables, such as precipitation (Sankaran et al., 2005), in addition to biogeochemical factors such as soil type and nutrient availability (Scholes and Walker, 1993). Rainfall for example is a key predictor in the seasonality of vegetation in this region (Chudimayo, 2001; Parrini and Erasmus, 2009; Higgins et al., 2011; February and Higgins 2016; Cho et al., 2017). Secondly, the KNP has a distinct geological pattern, which along with other factors, significantly determines the species diversity of flora and fauna (Venter and Gertenbach, 1983; Schutte, 1986; Scholes and Walker, 1993). In the western part of the park, woody vegetation grows on weathering-resistant coarse-grained igneous rock, while the eastern part is dominated by basalts and clayey soils that supports more grasses and herbaceous species (Schutte, 1986; Venter et al., 2003). Furthermore, there is a north-south rainfall gradient which also determines the types of vegetation found throughout the park (MacFadyen et al., 2018). The northern region of the park is dominated by Mopane woodland vegetation while the southern bioregion is a diverse mixed woodland (Venter and Gertenbach, 1986).

Understanding vegetation seasonality and how seasonality relates to climate variables is important for ascertaining the degree to which ecosystems are vulnerable to climate changes. However, monitoring of vegetation phenological patterns has mostly been done using field data and continuous flux tower monitoring which both cover a small spatial extent (Nickless et al., 2009; Whitecross et al., 2016; Masia et al., 2018). Remote sensing has, in recent years, provided a complementary alternative as it covers a larger spatial extent (Jin et al., 2013; Buitenwerf et al., 2015). A limited number of studies have made use of satellite derived vegetation indices (VIs) in order to analyse phenological patterns in the lowveld region and only a few have been conducted in the KNP (Archibald and Scholes, 2007; Parrini and Erasmus, 2009, Higgins et al., 2011). Vegetation indices (VIs) such as the Normalized Difference Vegetation Index (NDVI) are the most common tool used in phenology studies, however, they are proxies and thus are not a direct measure of vegetation productivity. The Fraction of Absorbed Photosynthetically Active Radiation (FAPAR) on the contrary is a biophysical measure of primary productivity which offers more ecologically relevant information in comparison to vegetation indices (Fensholt et al., 2004).

The continuous temporal coverage of the data allows us to describe vegetation seasonality trends and to understand how these patterns and trends varied within the landscape. found

that the proportions of tree cover in an area directly influences the phenological metrics computed for that area or the phenological response thereof (Higgins et al. 2007; Cho et al., 2017). Therefore, the separation of the landscape based on broad-scale geology and bioregions representative of different species composition and varying drivers of change could provide a better understanding of phenology in this complex system. Urban et al. (2020) shows that woody cover is generally higher in the granite region, while the basalt has a larger proportion of grass species which is also consistent with findings by Eckhardt et al. (2000). Furthermore, from 1998 to 2012, there were gains in both geologies in woody vegetation cover in the northern bioregion (>100% in basalts and 39% in granites), but losses in the southern region (29% in granites and 40 in basalts) (Munyati and Sinthumule, 2016). This study, therefore, aimed to describe and compare the spatio-temporal phenological patterns and trends between two broad-scale geologies (basalt and granite) and between two distinct bioregions (Mopane dominated northern region and the southern region) in the Kruger National Park using 18 years (2001 – 2018) of MODIS FAPAR data.

Recent studies showed that rainfall did not show significant directional trends between 1981 and 2015 (Van Wilgen et al., 2016; MacFadyen et al., 2018) and therefore I expected that the phenological metrics would also not show strong increasing or decreasing trends. However, because of the reported association between rainfall and phenology (Higgins et al., 2011; Whitecross et al., 2017), I hypothesised that an increase in rainfall variability may correlate with an increase in the variation of the phenology metrics over time. Due to the broad-scale differences in the vegetation functional types as represented by the geologies and the northern and southern bioregions, I postulated that between 2001 and 2018 a perceived earlier green-up on granite could be due to a higher proportion of trees as opposed to the basalt, but rainfall may further influence the seasonality. Also, due to the heterogenous nature of vegetation distribution in the park, I expected that there would be higher variability in the values of the phenology metrics for the more diverse southern bioregion as well as basalts in comparison to the Mopane dominated northern region and granites, respectively. Finally, I expected that in the absence of a strong influence of rainfall changes on landscape phenology, there would be localized change trends due to the well documented impact of elephants, herbivores and fire (Levick et al., 2009; Pellegrini et al., 2017).

2.3 Methods

2.3.1 Study Area

The Kruger National Park (Figure 1) is one of the largest and biophysically diverse protected areas in the world, located in the north-eastern corner of South Africa (Scholes and Walker, 1993). It falls in the lowveld savanna between 22° 20'S to - 25° 32' S and 30° 47'E to 32° 00' E with a spatial extent of around two million hectares (Du Toit *et al.,* 2003). The lowveld region is a low-lying landscape at 300 m above sea level with gentle slopes, however, the elevation of the KNP ranges between 260 m and 839 m. Long-term climatic data shows that the park experiences high mean summer temperatures (26.4 °C) with mild mean winter temperatures (9.5 °C) as well as seasonal variation in rainfall (van Wilgen *et al.,* 2016). In the last five decades the mean minimum and mean maximum temperatures have increased by 0.8 °C (van Wilgen *et al.,* 2016). The park experiences a rainfall gradient with the south-western part receiving an annual average of around 750 mm while the north eastern part receives 350 mm annual average (van Wilgen *et al.,* 2016). The northern bioregion of the KNP is dominated by Mopane while the southern bioregion is a diverse mixed woodland dominated by *Terminalia sericea* and *Dichrostachys cinerea* to the west and *Acacia (Senegalia) nigrescens* to the east (Venter and Gertenbach, 1986).

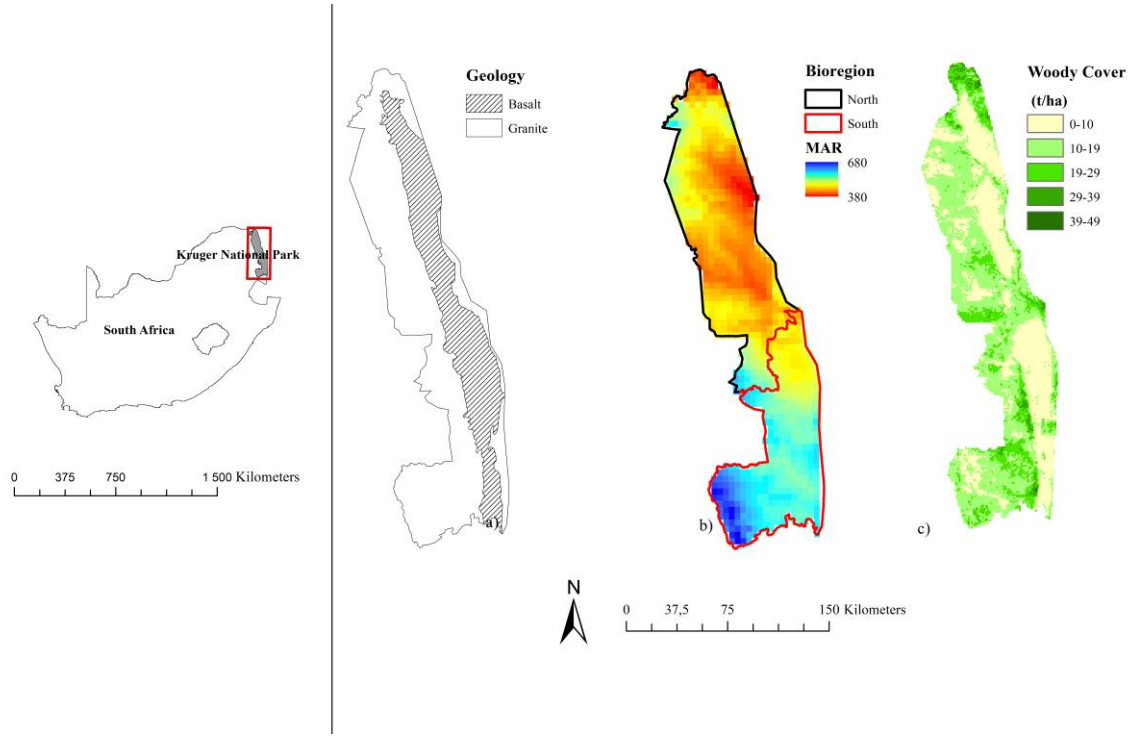


Figure 2.1: The Kruger National Park (KNP) is located in the most north eastern part of South Africa occupying two provinces (Limpopo and Mpumalanga). The park is (a) divided into two main geology types (Basalt and Granite) and (b) has a north-south rainfall gradient roughly representative of a northern Mopane bioregion that receives lower mean annual rainfall (MAR) and a southern mixed woodland bioregion that receives a higher MAR (2001 – 2017). The woody cover map by Urban et al. (2020) in (c) shows differences between the two main geologies due to differences in nutrient availability (Venter and Gertenbach, 1986).

2.3.2 MODIS and rainfall data

The MODIS fPAR product (MOD15A2H) that I used to describe and evaluate the phenological trends of the study area has an 8-day repeat cycle at 500 m spatial resolution and was acquired from the USGS Land Processes DAAC at EROS (https://search.earthdata.nasa.gov/). The MOD15A2H images from 2001 to 2018 were downloaded and re-projected from the MODIS sinusoidal projection to WGS84 UTM 36S in the MODIS conversion toolkit (MCTK) (White, 2019). I then extracted the fPAR and FPARLai_QC bands in ENVI IDL 8.5 (https://www.harrisgeospatial.com/Software-Technology/IDL). To analyse rainfall trends for the study period, I acquired 216 rainfall images at 21 km spatial resolution and a monthly temporal resolution from the WorldClim data website (https://www.worldclim.org/data/monthlywth.html). WorldClim provides

historical monthly weather data, downscaled from CRU-TS-4.03 (Harris et al., 2014) using WorldClim 2.1 (Fick and Hijmans, 2017) for bias correction.

2.3.3 Deriving phenological metrics

TIMESAT version 3.3 (Eklund and Jonsson, 2017) was used to derive phenology metrics from the MODIS fPAR time series in order to assess the phenological trends in the Kruger National Park. To reduce the noise of the time series data from outliers, curve fitting was done using the Savitzky Golay algorithm. This algorithm is robust and resistant to outliers which makes it useful for a noisy time series (Eklund and Jonsson, 2017).

TIMESAT offers other in-built algorithms for recognizing the thresholds of the fitted curve in order to estimate phenological metrics such as the start of season. I used the Seasonal Amplitude setting which requires the user to define FAPAR values at which a growing season starts and ends. This method determines the start of season when the left part of the fitted curve reaches a fraction of the amplitude based on the user-defined base level (Eklund and Jonsson, 2017). To determine these user-defined values for season start and end, I used the seasonal trend decomposition by Leoss (STL) method within TIMESAT (Ekhlund and Jonsson, 2017; Wang et al., 2019). The STL indicated that the start of season date was 10% over the minimum fPAR level (0.2 in this study) and that the end of season was 20% lower than the maximum fPAR level (0.7). Therefore, I defined the start of season as the point at which fPAR levels reached 30% which indicated the initial green-up and the end of season at 50% fPAR level where leaf senescence has set on.

Seasonality images of the different phenological metrics; Start of Season (SOS), Length of Season (LOS), End of Season (EOS), and the FAPAR Large integral (accumulated biomass -- Diouf et al., 2015) were generated from the fitted time series and weighted with quality data for the time period, 2001 to 2018. I specified the weights for the MODIS QC layer in TIMESAT. Values ranging from 0 - 7 were good quality data and were given a weight of 1, and values ranging from 8 – 157 were treated as bad values and were given a weight of 0.1. The output seasonality images from TIMESAT were then spatially referenced and converted into 16-bit images using IDL 8.5 and SPIRITS GIS (http://www.un-spider.org/links-and-resources/gis-rs-software/spirits-jrc) for use in ArcMap 10.5 (https://support.esri.com/en/products/desktop/arcgis-desktop/arcmap/10-5).

2.3.4 Data Analysis

To determine if there were any change trends in each of the metrics over the study period, I analysed the mean and variation (standard deviation) of the phenological metrics and rainfall over the time period using linear regression. These time series trends were compared between the geology types (basalt and granite) and between the two bioregions (north and south) with post-hoc ANOVA analyses. I then tested for the difference in the mean and variation of the phenological metrics between the two geologies and the two bioregions using a student's t-test. To further investigate the spatial extent of the possible trends, I used the Curve Fit extension tool (https://www.umesc.usgs.gov/management/dss/curve_fit.html) for ArcGIS to apply a pixel level linear regression of the phenological metrics over the time series from 2001 – 2018. The output were raster maps of the slope, the correlation coefficient, and p-value for each pixel. For each metric I calculated a final raster map showing pixels with significant increasing or decreasing linear trends across the KNP landscape that satisfied the conditions of equation 2.1 and equation 2.2.

$$\textit{Significant positive trend} = R^2 > 0.5,\ p < 0.05 \text{ and slope} > 0 \qquad \textbf{(Equation 2.1)}$$

$$\textit{Significant negative trend} = R^2 > 0.5,\ p < 0.05 \text{ and slope} < 0 \qquad \textbf{(Equation 2.2)}$$

I then calculated the percentage of change (*%Δ)* for all the metrics to determine how much change has occurred within each of the different bioregions and geologies using equation 2.3. Additionally, I calculated the percentage of change (*%Δ)* of each metric throughout the entire park using equation 2.4.

$$\%\Delta \textit{ within geology or bioregion} = [\textit{Area } (km^2) \textit{ with significant trend}] / [\textit{total geology or bioregion area } (km^2)] * 100 \qquad \textbf{(Equation 2.3)}$$

$$\%\Delta \textit{ across KNP} = [\textit{Area } (km^2) \textit{ with significant trend}] / [\textit{total KNP area } (km^2)] * 100 \qquad \textbf{(Equation 2.4)}$$

2.4 Results

2.4.1 Geology comparison of vegetation phenological metrics and trends

Over the 18-year study period, there was no significant change trend in all the metrics for both geologies (Figure 2.2) except for the basalt vegetation that showed a significant

decreasing trend in the variation of SOS (Figure 2.2b). Rainfall also did not show any significant change trend over the 18-year study period in each of the geologies (Figure 2.2i).

Comparison between the two geologies indicated that the means of all the metrics and the standard deviations were significantly different during the study period. On average, the growing season (SOS) started in composite 41 (third week of November), and 42 (first week of December) for the basalt and granite geologies respectively, with a statistically significant earlier onset (t-test: $t=12$, $d.f=16$, $p<0.05$) of about 7-10 days across the study period in the basalt geology (Fig 2.2a and 2.2b). The LOS was significantly longer in the granite geology by about 4 - 17 days (t-test: $t=9$, $d.f.=16$, $p<0.001$), while the basalt vegetation showed larger variation in season length (t-test: $t=8$, $d.f.=16$, $p<0.001$).

On average, the growing season ended 7-14 days earlier in the basalt (mid-June) than in the granite geology (late June) between 2001 and 2018 (t-test: $t=-7$, $d.f.=16$, $p<0.001$). The basalt geology had a higher average large integral value (t-test: $t=-16$, $d.f.=16$, $p<0.001$). Similarly, there was a significant difference in annual average rainfall between the two geologies with the granite geology receiving about 40 mm more rainfall across the study period (t-test: $t=-19$, $d.f.=16$, $p<0.001$).

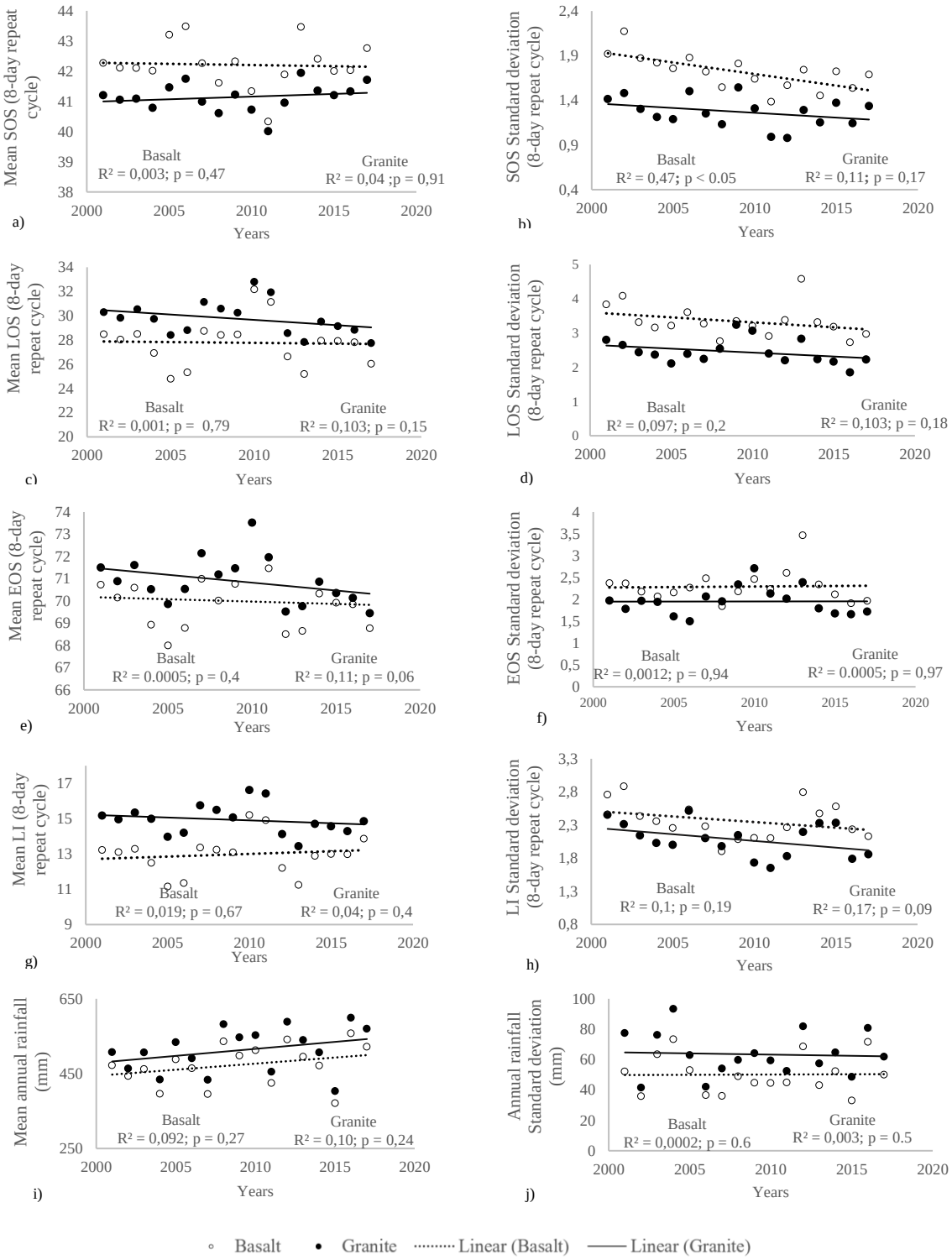


Figure 2.2 : Comparison of (a) mean start of season (SOS), (b) SOS variation, (c) mean length of season (LOS), (d) LOS variation, (e) mean end of season (EOS), (f) EOS variation, (g) mean large integral, (h) large integral variation, (i) mean annual rainfall as well as (j) mean rainfall variation between the basalt and granite geologies over an 18 year period (2001 – 2018) in the Kruger National Park.

2.4.2 Bioregion comparison of vegetation phenological metrics and trends

Both the north and the south bioregions showed no significant change trend in the means and variation over the study period for most of the phenological metrics (Figure 2.3 a, c, f-h) as well as for rainfall (Figure 2.3i-j). Some exceptions where I observed a statistically significant linear time series trend include; a decreasing trend of the mean EOS in the south (Figure 3e) as well as decreasing trends in SOS variation (Figure 3b) and LOS variation (Figure 3d) in the north.

Comparison of the phenological metrics between the north and south bioregions, however, indicated a more consistent significant difference over the study period for most of the metrics except for the LOS ($p = 0.15$). Specifically, the mean SOS was significantly later in the northern region where the growing season started on average in composite 42 (the first week of December) compared to composite 40 (the second week of November) in the southern region (t-test, $t=11$, d.f.=16, $p<0.001$). The variation in the SOS was also higher in the northern region (t-test: $t=3$, d.f.=16, $p<0.001$). Both bioregions showed similar LOS with just a 3-5-day difference between the north and south (t-test: $t=1$, d.f=16, $p=0.07$) (Figure 2.3c), but the variation in LOS was significantly higher in the north (t-test: $t=2$, d.f.=16, $p=0.02$).

The growing season ended significantly later in the northern region in composite 71 (late June) compared to the southern region (composite 70/mid-June) (t-test: $t= 7$, d.f.=16, $p<0.001$). The mean and variation of LI were significantly higher in the southern region in comparison to the northern region (t-test, $t=-7$, d.f.=16, $p<0.001$). Finally, the northern region of the Kruger National Park received 90 mm less rainfall which was significantly less than the southern region (t-test: $t=14$, d.f=16, $p<0.001$)

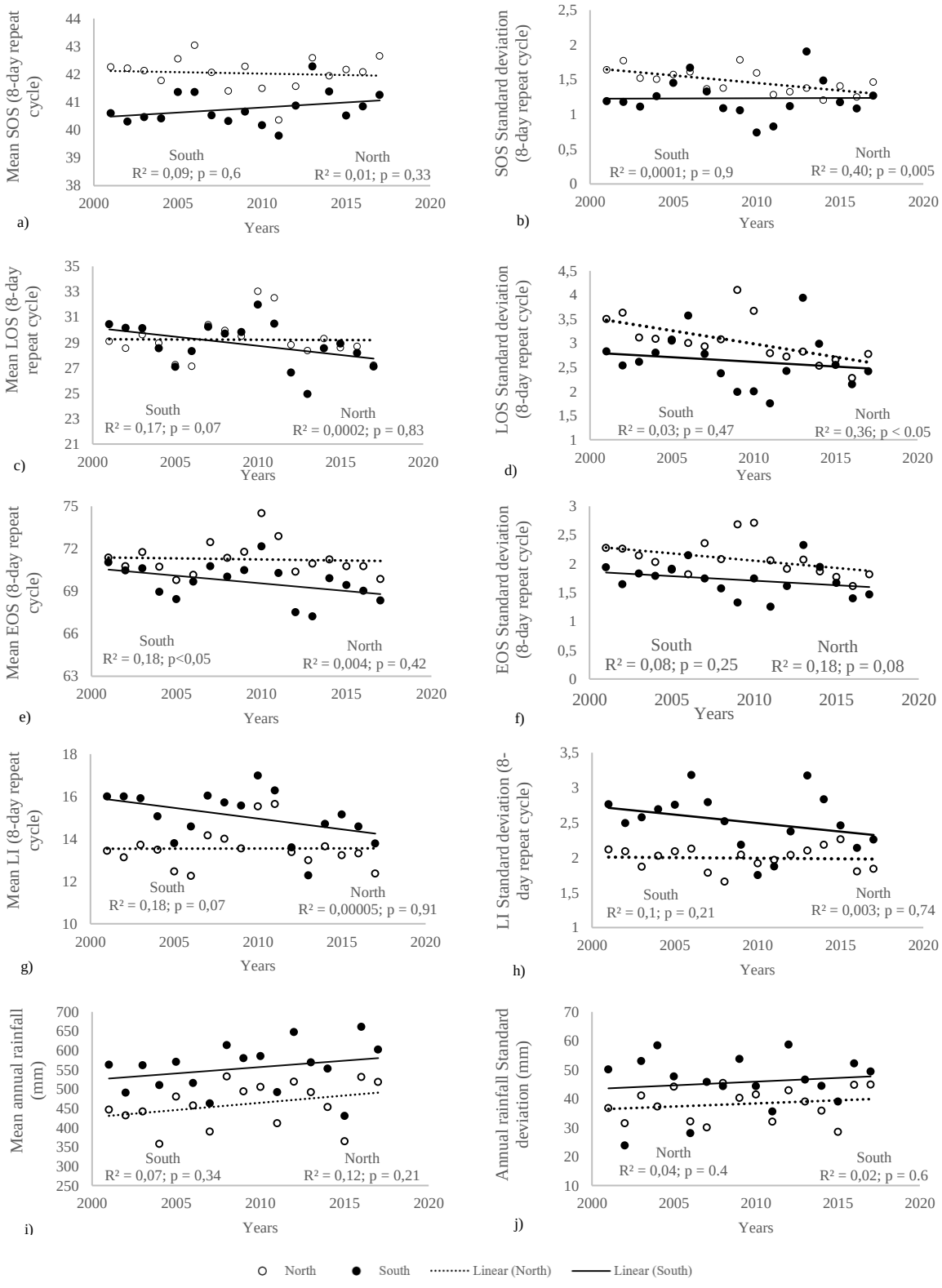


Figure 2.3: Comparison of (a) mean start of season, (b) start of season variation, (c) mean length of season, (d) length of season variation, (e) mean end of season, (f) end of season variation, (g) mean large integral, (h) large integral variation (i) mean annual rainfall, as well as the (j) mean rainfall variation between the north and south bioregions over an 18 year period (2001 – 2018) in the Kruger National Park.

2.4.3 Pixel-level raster regression

Over the study period, there were statistically significant localized linear trends in all the phenological metrics within the KNP (Figure 2.4). In several localized areas in the north and north eastern parts of the park, the SOS came earlier (Figure 2.4a), while the end of season came later (Figure 2.4b). In these localized northern parts, the LOS was longer coinciding also with an increase of the large integral values over the study period (Figure 2.4c and d). The opposite can be observed for the south and south western parts of the park where the growing season came significantly later and ended earlier in certain localities (Figure 2.4a and b). The spatial extent of these trends also overlapped with a shorter LOS and a decrease in the large integral value over the study period.

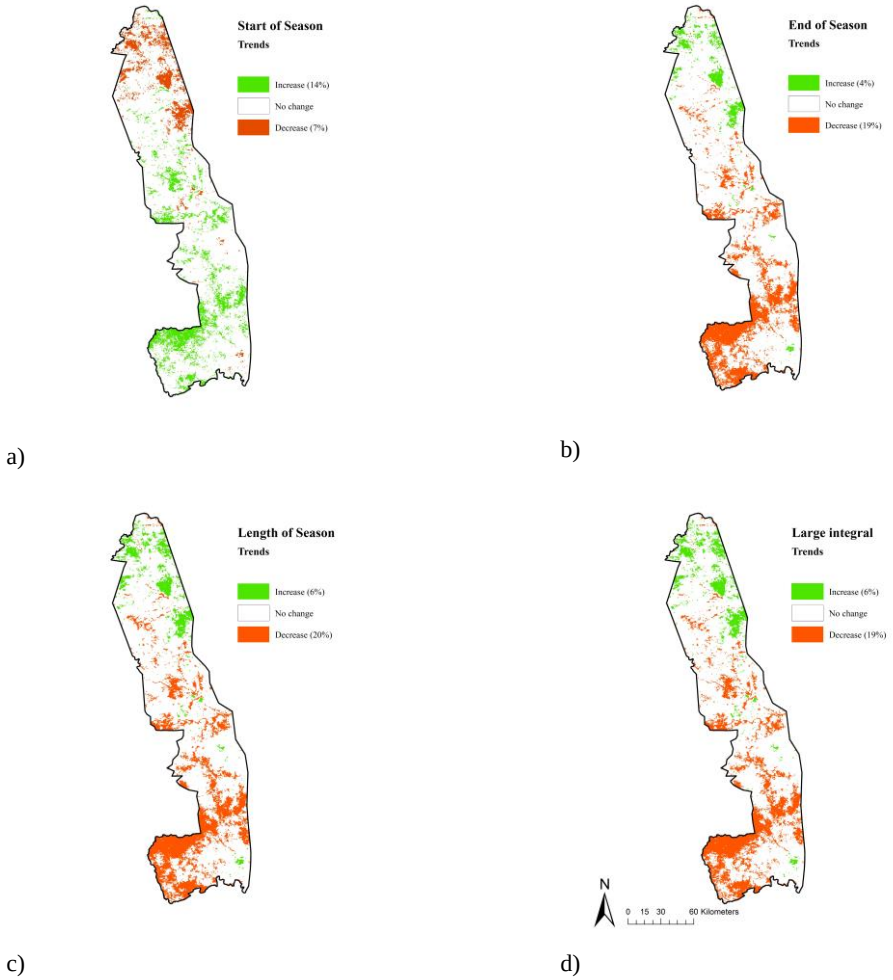


Figure 2.4: Pixel level raster regression of a) Start of season, b) End of season, c) Length of season and d) the large integral in the Kruger National Park for a period of 18 years (2001 – 2018). The green symbols indicate a significant increase whereby $R^2 > 0.5$, $p < 0.05$ and slope >0, and the red symbols indicate a significant decrease whereby $R^2 > 0.5$, $p < 0.05$ and slope <0.

The southern region experienced the most change (31.8%) in vegetation seasonality while the northern region is experiencing the least (18.3%) (Table 2.1a). Across all metrics, and between the two geologies, more change can be attributed to the granite (16%) compared to the basalt (7%) in the KNP (Table 2.1b). Most of the localized increases in SOS occurred in the southern bioregion (24%) while the decreases in SOS mainly occurred in the northern region (11%).

Table 2.1: Percentage change within (1) granite geology, (2) basalt geology, (3) north region, and (4) the southern region over an 18-year period (2001 – 2018) in the Kruger National Park, South Africa.

Phenological metric	Change	Granite %	Basalt %	North %	South %
SOS	Increase	16,2	9,9	7,5	24,2
	Decrease	4,4	10,5	10,7	0,6
	Total	**20,5**	**20,4**	**18,3**	**24,8**
LOS	Increase	3,9	10,4	10,4	0,5
	Decrease	23,8	12,9	9,5	34,6
	Total	**27,7**	**23,3**	**19,8**	**35,1**
EOS	Increase	2,5	7,3	6,8	0,5
	Decrease	22,2	12,1	8,2	33,5
	Total	**24,7**	**19,4**	**15,0**	**33,9**
LI	Increase	4,1	11,0	10,9	0,7
	Decrease	22,4	12,4	9,2	32,6
	Total	**26,5**	**23,4**	**20,1**	**33,3**
	Mean	**24,9**	**21,6**	**18,3**	**31,8**

Table 2.2: Attribution of change (%) by the (1) granite geology, (2) basalt geology, (3) north region, and (4) the southern region to the total changes across the Kruger National Park over an 18-year period (2001 – 2018)

Phenological metric	Change	Granite %	Basalt %	North %	South %
SOS	Increase	9,2	3,1	4,0	8,2
	Decrease	2,9	3,5	6,2	0,2
	Total	**12,1**	**6,6**	**10,2**	**8,4**
LOS	Increase	2,5	3,2	5,4	0,2
	Decrease	15,7	4,4	5,5	14,5
	Total	**18,2**	**7,6**	**10,9**	**14,7**
EOS	Increase	1,6	2,3	3,7	0,2
	Decrease	14,6	4,1	4,7	14,0
	Total	**16,2**	**6,4**	**8,4**	**14,2**
LI	Increase	2,6	3,4	5,7	0,3
	Decrease	14,8	4,2	5,3	13,7
	Total	**17,4**	**7,6**	**11,0**	**14,0**
	Total	**15,9**	**7,0**	**10,1**	**12,8**

2.5. Discussion

This study sought to investigate the possible differences in vegetation phenological trends between two distinct geology types (granite and basalt) and between the Mopane-dominated northern region and the *Acacia nigrescens* dominated southern region over the last two decades in the Kruger National Park. An earlier EOS for the southern bioregion was the only significant change trend between 2001 and 2018. However, changes in the variation of some of the phenometrics were evident, with the basalt vegetation showing decreases in the variation of SOS and the northern Mopane-dominated region showing decreases in variation for both SOS and LOS.

Over the same period, rainfall showed no significant increasing or decreasing trends at both the landscape scale and localized scale. It is important to note that the spatial resolution of the

rainfall data was very coarse (21 km pixel) and was not able to pick up local variations in rainfall at the same spatial scale of the phenology metrics. Rainfall is coupled to biogeochemical factors that result in suitable conditions for varied vegetation functional types. These may be reflected by the differences in vegetation functional types and tree-grass ratios between the bioregions and between the geologies. In addition, rainfall has an impact on soil moisture which has been shown to be a more direct driver of phenology for both trees and grasses (Archibald and Scholes, 2007). Therefore, changes in rainfall over time would be expected to induce changes in vegetation phenology response and or distribution over time. However, rainfall has also been shown to fall short at describing phenology patterns/trends because it may not reflect the continuous water balance but rather an input into the system (Archibald and Scholes, 2007).

EOS is related to leaf senescence and differs vastly between different species. It is largely driven by soil moisture for both grass and tree species (Higgins et al., 2011). Additionally, leaf senescence can also be affected by changes in temperature (Higgins et al., 2011), day length (Higgins et al., 2011), and herbivory (Rossatto et al., 2009). It is possible that the earlier EOS in the southern region is a consequence of localized declines in MAR at a much finer spatial scale than the one assessed in this study. There has also been an increase in the frequency and intensity of drought events in the savanna region that are causing low levels of moisture more frequently and for longer periods (Case et al., 2019). This has been shown to result in less time in which vegetation is photosynthetically active and thus the period in which leaves remain green (Higgins et al., 2011; Devine et al., 2017). While soil moisture reduction induced by drought would affect the entire Kruger landscape to some extent, northern woody species are more adapted to low and more variable soil moisture levels compared to the southern species that receive higher MAR (~ 750 mm) (Viljoen, 1995).

There were some negative change trends in LOS and LI (accumulated biomass) in the southern region even though they were not statistically significant. It is likely that the change trend of LOS and LI might intensify in the future should the frequency and severity of drought conditions and climate change increase. Additionally, I did the analysis at a landscape level whereby it may take a longer period for broad-scale long term changes to be displayed. SOS did not show any significant change trend over the study period. Higgins et al. (2011) suggested that the SOS is driven largely by day length and or photoperiod in tree species in the savanna while grasses rely on an increase of soil moisture from the summer

rains. Long term changes in soil moisture, might not be occurring at a rate that would cause significant changes in SOS at the temporal or spatial resolution at which I did the analysis.

Comparison of the phenology metrics between the bioregions and between the geologies showed distinct differences in the means and variation over the study period. As expected, the granite geology and the northern bioregion, representative of higher woody vegetation cover, consistently displayed an earlier SOS, and later EOS compared to their counterparts with lower woody cover at the landscape scale (Schutte, 1986; Staver et al., 2017). These findings therefore also support the conclusions by Cho et al. (2017) who showed that areas with a larger proportion of tree cover show an earlier growing season. Woody species in a water limited savanna have adaptations such as the ability to store carbohydrates and carbon belowground along longer roots that can reach deeper water resources than grasses (Choat et al., 2018). This allows tree species to green-up early when compared to grasses and other herbaceous species that depend on the first summer rains for their initial green-up (Archibald and Scholes, 2007; February and Higgins, 2016). Woody species also keep their leaves green for longer by utilizing stored resources while grasses may reach abscission early, resulting in woody vegetation having longer LOS and later EOS (Archibald and Scholes, 2007; Higgins et al., 2011).

Additionally, the larger variation in the basalt geology for all the metrics could be ascribed to a greater temporal separation between tree and grass phenology (Cho et al., 2017). These findings suggest that there are broad-scale differences in phenology in the Kruger National Park, corresponding to the vegetation types and structural heterogeneity in the different geologies and bioregions.

The northern bioregion is dominated by a woody Mopane species which tends to flush its leaves after the first summer rains, usually during October (Makhado, 2018). Meanwhile a dominant southern species (*Acacia nigresens)* greens up significantly earlier (Archibald and Scholes, 2007). Therefore, the later growing season in the southern region could be ascribed to other species that green-up late such as grasses and the *Combretum* species (~16 November) (Archibald and Scholes, 2007). I had expected the variation to be higher in the southern region due to different seasonal responses caused by higher heterogeneity since it is a mixed woodland. It has also been shown that the southern region has experienced gains in grass species and a loss of tree species (Munyati and Sinthumule, 2016). However, this was

not the case and the variation may suggest a more diverse phenological response from the Mopane species.

The pixel level analysis showed clear change trends at a localized level. In the northern bioregion, localized advancement of SOS that spatially coincided with longer LOS, delayed EOS and increasing LI values were prominent and indicated increasingly productive growth seasons. In the southern bioregion, however, the growth season became less productive over the study period as change trends in localised areas were dominated by delayed SOS, shorter LOS, earlier EOS and decreasing LI values. From a landscape perspective, these diverging change trends may be indicative of vegetation structural changes that resulted from several interconnected processes such as localized changes in rainfall, herbivory, and fire.

Areas with more woody vegetation compared to areas dominated by grasses tend to have earlier SOS, a longer LOS and a later EOS similar to the phenological pattern of the northern region (Cho et al., 2017). These results support that there has been a gain in woody vegetation over time in the northern region (Munyati and Sinthumule, 2016). Top down factors such as limited herbivory and shorter fire return periods may be driving this particular change in vegetation proportion along with bottom up factors such as climate and changes in carbon dioxide (Devine et al., 2017). February et al. (2013) showed that localized sequences of low rainfall, intense grazing and temporary droughts decrease tree-grass competition allowing for rapid woody growth (Devine et al., 2017). Combined, these factors also reduce the fuel load, allowing for tree species to escape the fire trap (Devine et al., 2017) resulting in a positive feedback.

Woody vegetation species that grow in higher-rainfall regions such as the southern bioregion are inferior competitors to grass species for soil moisture (February et al., 2013). Besides soil moisture, other factors such as herbivory tend to increase competition from grasses resulting in less growth of woody vegetation (February et al., 2013). Similarly, shorter fire return periods result in tree species not being able to escape the fire trap under these conditions leading to a positive feedback loop that increases the proportion of grasses over time (Devine et al., 2017). Alternatively, elephants (*Loxodonta africana)* could also play an important role in the localized removal of woody cover in the southern region (Case et al., 2019). All these factors could be interactively contributing to a less productive growth season through the reduction of woody vegetation in the southern region.

The per-pixel landscape analysis suggested that in the southern region, negative change trends in LOS and LI may become significant over the next decade as well as a more apparent north-south-gradient difference in change trends.

Bunting et al. (2018) showed that the loss of woody vegetation in the southern region could be offset by the gain in the northern region. This might not be the case given the amount of localized negative change (19%) that is apparent in accumulated biomass in the southern region compared to the localized positive gains (6%) in the northern region. Archibald et al., (2009) further stresses how important the presence of green leaves is to Net Ecosystem Exchange (NEE) and generally the amount of biomass that can store that carbon. The decrease in length of season shown by the pixel level analysis, means that the overall time in which vegetation is photosynthetically active might decrease and therefore the amount of time in which the system is a sink could also decrease. Similarly, the overall loss of biomass could result in less aboveground carbon stored in the landscapes (Archibald et al., 2009). Archibald et al. (2009) concluded that the variability of NEE at the Skukuza flux site within the Kruger National Park is largely controlled by length of time that leaves are displayed by trees and grasses. Therefore, I propose that the relationship between the seasonality, especially length of season and accumulated biomass, and NEE needs to be studied and understood in this system in order to be able to accurately quantify and model the carbon stock over the entire landscape.

In conclusion, the findings of this study show that at a landscape level, rainfall and phenology metrics did not change significantly over time except for the EOS in the northern region. The lack of clear change trends might be due to the relatively short temporal coverage of the study period combined with the coarse spatial scale at which the analysis was done. Secondly, the phenology responses between the bioregions and between the geologies were consistently different. This indicates that the differences in factors such as rainfall, soil moisture availability, nutrient availability amongst others between the geologies and bioregions influences the vegetation functional types within these landscapes and thus the phenology response. Thirdly this study suggests that there were localized change trends likely due to top-down factors such as fire and herbivory. This is highlighted by the localized and concurrent change trends in SOS, EOS, LI and LOS coinciding spatially. Lastly the study showed that a large area of the Kruger National Park experienced shorter length of seasons and a reduction in biomass and this has a potential to shorten the carbon sequestration period by aboveground biomass.

2.6. References

Archer, E.R., Engelbrecht, F.A., Hänsler, A., Landman, W., Tadross, M. and Helmschrot, J., 2018. Seasonal prediction and regional climate projections for southern Africa. In *Climate change and adaptive land management in southern Africa – assessments, changes, challenges, and solutions,* pp. 14-21 Klaus Hess Publishers.

Archibald, S. A., Kirton, A., van der Merwe, M. R., Scholes, R. J., Williams, C. A., and Hanan, N. 2009. Drivers of inter-annual variability in net ecosystem exchange in a semi-arid savanna ecosystem, South Africa. *Biogeosciences*, 6, pp. 251–266.

Archibald, S. and Scholes, R.J., 2007. Leaf green-up in a semi-arid African savanna-separating tree and grass responses to environmental cues. *Journal of Vegetation Science*, *18*(4), pp.583-594.

Bunting, E.L., Fullman, T., Kiker, G. & Southworth, J., 2016. Utilization of the SAVANNA model to analyse future patterns of vegetation cover in Kruger National Park under changing climate. *Ecological Modelling* 342: 147-160.

Bunting, E.L., Munson, S.M. and Bradford, J.B., 2019. Assessing plant production responses to climate across water-limited regions using Google Earth Engine. *Remote Sensing of Environment*, *233*, p.111379.

Case, M.F., Wigley-Coetsee, C., Nzima, N., Scogings, P.F. and Staver, A.C., 2019. Severe drought limits trees in a semi-arid savanna. *Ecology*, *100*(11), p.e02842.

Cho, M.A., Ramoelo, A. and Dziba, L., 2017. Response of land surface phenology to variation in tree cover during green-up and senescence periods in the semi-arid savanna of Southern Africa. *Remote Sensing*, *9*(7), p.689.

Choat, B., Brodribb, T.J., Brodersen, C.R., Duursma, R.A., Lopez, R. and Medlyn, B.E., 2018. Triggers of tree mortality under drought. *Nature*, *558*(7711), pp.531-539.

Chidumayo, E.N., 2001. Climate and phenology of savanna vegetation in southern Africa. *Journal of Vegetation Science*, pp.347-354.

Devine, A.P., McDonald, R.A., Quaife, T. and Maclean, I.M., 2017. Determinants of woody encroachment and cover in African savannas. *Oecologia*, *183*(4), pp.939-951.

Diouf, A.A., Brandt, M., Verger, A., Jarroudi, M.E., Djaby, B., Fensholt, R., Ndione, J.A. and Tychon, B., 2015. Fodder biomass monitoring in Sahelian rangelands using phenological metrics from FAPAR time series. *Remote Sensing*, *7*(7), pp.9122-9148.

Dragoni, D., Schmid, H.P., Wayson, C.A., Potter, H., Grimmond, C.S.B. and Randolph, J.C., 2011. Evidence of increased net ecosystem productivity associated with a longer vegetated season in a deciduous forest in south-central Indiana, USA. *Global Change Biology*, *17*(2), pp.886-897.

Du Toit, J.T., Rogers, K.H. and Biggs, H.C., 2003. Vegetation dynamics in the Kruger ecosystem, In *The Kruger experience: ecology and management of savanna heterogeneity*, Island Press. *Washington, DC, US*.

Dube, K. and Nhamo, G., 2019. Climate change and potential impacts on tourism: evidence from the Zimbabwean side of the Victoria Falls. *Environment, Development and Sustainability*, *21*(4), pp.2025-2041.

Eckhardt, H., Van Wilgen, B.W. and Biggs, H., 2000, 'Trends in woody vegetation cover in the Kruger National Park, South Africa, between 1940 and 1998', *African Journal of Ecology* 38(2), 108–115.

Eklundh, L. and Jönsson, P.T., 2017. 3.3 with Seasonal Trend Decomposition and Parallel Processing—Software Manual. *Lund University: Lund, Sweden*, p.88.

Ernst, Y.M., 2018. *Spatio-temporal trends in vegetation dynamics across a savanna-dominated national park* (Doctoral dissertation).

February, E.C., Higgins, S.I., Bond, W.J. and Swemmer, L., 2013. Influence of competition and rainfall manipulation on the growth responses of savanna trees and grasses. *Ecology*, *94*(5), pp.1155-1164.

February, E.C. and Higgins, S.I., 2016. Rapid leaf deployment strategies in a deciduous savanna. *PloS one*, *11*(6), p.e0157833.

February, E., Pausch, J. and Higgins, S.I., 2020. Major contribution of grass roots to soil carbon pools and CO 2 fluxes in a mesic savanna. *Plant and Soil*, *454*(1), pp.207-215.

Fensholt, R., Sandholt, I. and Rasmussen, M.S., 2004. Evaluation of MODIS LAI, fAPAR and the relation between fAPAR and NDVI in a semi-arid environment using in situ measurements. *Remote sensing of Environment*, *91*(3-4), pp.490-507.

Fick, S.E. and Hijmans, R.J., 2017. WorldClim 2: new 1-km spatial resolution climate surfaces for global land areas. *International journal of climatology*, *37*(12), pp.4302-4315.

Harris, I.P.D.J., Jones, P.D., Osborn, T.J. and Lister, D.H., 2014. Updated high-resolution grids of monthly climatic observations–the CRU TS3. 10 Dataset. *International journal of climatology*, *34*(3), pp.623-642.

Higgins, S.I., Delgado-Cartay, M.D., February, E.C. and Combrink, H.J., 2011. Is there a temporal niche separation in the leaf phenology of savanna trees and grasses? *Journal of Biogeography*, *38*(11), pp.2165-2175.

Jin, C., Xiao, X., Merbold, L., Arneth, A., Veenendaal, E. and Kutsch, W.L., 2013. Phenology and gross primary production of two dominant savanna woodland ecosystems in Southern Africa. *Remote Sensing of Environment*, 135, pp.189-201.

Jones, L.A., Kimball, J.S., Reichle, R.H., Madani, N., Glassy, J., Ardizzone, J.V., Colliander, A., Cleverly, J., Desai, A.R., Eamus, D. and Euskirchen, E.S., 2017. The SMAP Level 4 Carbon Product for Monitoring Ecosystem Land–Atmosphere CO 2 Exchange. *IEEE Transactions on Geoscience and Remote Sensing*, *55*(11), pp.6517-6532.

Keenan, T.F., Gray, J., Friedl, M.A., Toomey, M., Bohrer, G., Hollinger, D.Y., Munger, J.W., O'Keefe, J., Schmid, H.P., Wing, I.S. and Yang, B., 2014. Net carbon uptake has increased through warming-induced changes in temperate forest phenology. *Nature Climate Change*, *4*(7), pp.598-604.

Levick, S. R., Asner, G. P., Kennedy-Bowdoin, T., & Knapp, D. E. (2009). The relative influence of fire and herbivory on savanna three-dimensional vegetation structure. Biological Conservation, 142(8), 1693-1700.

MacFadyen, S., Hui, C., Verburg, P.H. and Van Teeffelen, A.J., 2016. Quantifying spatiotemporal drivers of environmental heterogeneity in Kruger National Park, South Africa. *Landscape Ecology*, *31*(9), pp.2013-2029.

MacFadyen, S., Zambatis, N., Van Teeffelen, A.J. and Hui, C., 2018. Long-term rainfall regression surfaces for the Kruger National Park, South Africa: a spatio-temporal

review of patterns from 1981 to 2015. *International Journal of Climatology*, *38*(5), pp.2506-2519.

Makhado, R.A., Potgieter, M.J. and Luus-Powell, W.J., 2018. Colophospermum Mopane Leaf Production and Phe-nology in Southern Africa's Savanna Ecosystem-A Review. *Insights For Res*, *2*(1), pp.84-90.

Masia, N.D., Stevens, N. and Archibald, S., 2018. Identifying phenological functional types in savanna trees. *African Journal of Range and Forage Science*, *35*(2), pp.81-88.

Munyati, C. and Sinthumule, N.I., 2016. Change in woody cover at representative sites in the Kruger National Park, South Africa, based on historical imagery. *SpringerPlus*, *5*(1), p.1417.

Nickless, A., Archibald, S.A., Van der Merwe, M.R., Scholes, R.J., Williams, C.A. and Hanan, N., 2011. Estimation of net ecosystem exchange at the Skukuza flux site, Kruger National Park, South Africa.

Parrini, F. and Erasmus, B.F.N., 2009. Spatial and temporal heterogeneity of phenology patterns in Kruger National Park, South Africa: different drivers for different areas. In *Proceedings, 33rd International Symposium on Remote Sensing of Environment, ISRSE* (Vol. 2009, pp. 627-631).

Pellegrini, A. F., Pringle, R. M., Govender, N., & Hedin, L. O. (2017). Woody plant biomass and carbon exchange depend on elephant-fire interactions across a productivity gradient in African savanna. Journal of Ecology, 105(1), 111-121.

Rossatto, D.R., Hoffmann, W.A. and Franco, A.C., 2009. Differences in growth patterns between co-occurring forest and savanna trees affect the forest–savanna boundary. *Functional Ecology*, *23*(4), pp.689-698.

Sankaran, M., Hanan, N. P., Scholes, R. J., Ratnam, J., Augustine, D. J., Cade, B. S., ... & Zambatis, N. (2005). Determinants of woody cover in African savannas. *Nature*, 438(7069), 846-849.

Scholes, R.J. and Walker, B.H. 1993. *An African savanna: a synthesis of the Nylsvlei study.* Cambridge University Press, Cambridge, UK.

Schutte, I.C., 1986. The general geology of the Kruger National Park. *Koedoe*, *29*(1), pp.13-37.

Simioni, G., Gignoux, J., Le Roux, X., Appé, R., Benest, D., 2004. Spatial and temporal variations in leaf area index, specific leaf area and leaf nitrogen of two co-occurring savanna tree species. *Tree Physiology 24*, 205–216.

Staver, A.C., Botha, J. and Hedin, L., 2017. Soils and fire jointly determine vegetation structure in an African savanna. *The New phytologist*, *216*(4), p.1151.

Urban, M., Heckel, K., Berger, C., Schratz, P., Smit, I.P., Strydom, T., Baade, J. and Schmullius, C., 2020. Woody cover mapping in the savanna ecosystem of the Kruger National Park using Sentinel-1 C-Band time series data. *koedoe*, *62*(1), pp.1-6.

Van Wilgen, N.J., Goodall, V., Holness, S., Chown, S.L. and McGeoch, M.A., 2016. Rising temperatures and changing rainfall patterns in South Africa's national parks. *International Journal of Climatology*, *36*(2), pp.706-721.

Venter, F.J. and Gertenbach, W.P.D., 1986. A cursory review of the climate and vegetation of the Kruger National Park. *Koedoe*, *29*(1), pp.139-148.

Viljoen, A.J., 1995. The influence of the 1991/92 drought on the woody vegetation of the Kruger National Park. *Koedoe*, *38*(2), pp.85-97.

Whitecross, M.A., Witkowski, E.T.F. and Archibald, S., 2017. Savanna tree-grass interactions: A phenological investigation of green-up in relation to water availability over three seasons. *South African Journal of Botany*, *108*, pp.29-40.

Chapter 3

3. Matching land surface phenology with the phenology of net ecosystem exchange (NEE) in the Kruger National Park, South Africa.

3.1 Abstract

Vegetation phenology plays a large role in driving the inter-annual variability of Net Ecosystem Exchange (NEE). However, in the Southern African region, the relationship between vegetation phenology and NEE is not well elucidated. Additionally, our understanding of Carbon Flux Phenology (CFP) in the region is limited by the sparse spatial coverage of flux tower sites. This study, therefore, aimed to assess and establish the relationship between Land Surface Phenology (LSP) using MODIS/MISR-HR FAPAR (Fraction of Photosynthetically Active Radiation) and Eddy Covariance Carbon Flux Phenology using 18 years of flux data at the Skukuza flux tower site, Kruger National Park. Cross-correlation results showed that there is a relatively strong association between FAPAR and NEE from both sensors (MISR-HR, $R^2 = 0.54$; MODIS, $R^2 = 0.53$) albeit with at least an 8-day lag in which FAPAR leads NEE. The linear regression showed that only the start of carbon uptake (SOS_{NEE}) has a strong correlation with FAPAR derived start of season ($SOS_{FAPAR)}$. In this analysis, MISR-HR FAPAR performed better at estimating the SOS_{NEE} dates ($R^2 = 0.61$) when compared to MODIS ($R^2 = 0.28$) and overall showed the least difference to CFP (Mean signed difference ~ 7 – 12 days). My findings showed that FAPAR data from MISR-HR, despite having more than 60% missing values, can be successfully used to approximate the SOS_{NEE} as well as NEE. The findings further indicated that a method that considers the intra-seasonal variation of NEE is needed when estimating CFP for future studies. In summary, this study presents insight into the relationship between LSP and CFP that contributes to our understanding of how LSP can be used to assist monitoring of carbon dynamics.

Keywords: Net ecosystem exchange, Land surface phenology, Carbon flux phenology, FAPAR, MODIS, MISR-HR

3.2 Introduction

Vegetation phenology plays a large role in the inter-annual variability of Net Ecosystem Exchange (NEE) through the direct impact it has on Gross Primary Productivity (GPP) (Zhu et al., 2013; Balzarolo et al., 2015). Indeed, variability of NEE is largely explained by the length of time that green leaves are displayed by vegetation in the savanna region (Archibald et al., 2009). Other studies also support this observation, noting that an earlier and/or later end of growing season extends the period in which vegetation is photosynthetically active and therefore results in a longer Carbon Uptake Period (CUP) (Jolly and Steven, 2004; Chuine, 2010; Zhang et al., 2011; Balzarolo et al., 2016).

There are two primary approaches used to study vegetation phenology. In-situ phenology includes ground-based observations such as visual monitoring and phenocams, as well as eddy-covariance flux-based data sources (Garrity et al., 2011). Alternatively, recurring seasonal patterns studied in vegetated land surface at a landscape or global scale through space-borne earth observation or remote sensing is referred to as Land Surface Phenology (LSP) (Gessner *et al.,* 2015). LSP is often characterised with parameters such as the start of season (SOS), length of season (LOS) and the end of season (EOS) among others. Phenology of NEE, also called CFP is represented by the timing at which NEE changes from a source to a sink and vice versa (Verma *et al.,* 2014; Balzarolo *et al.,* 2016). This consists of the start of carbon uptake (SCU) and end of carbon uptake (ECU). However, McCombs et al. (2018) showed that NEE phenology can also be estimated using the same approach as LSP. Zhu et al. (2013) observed that CUP, while controlled by LOS, is not identical to LOS and that the CUP will typically start or terminate before or after LSP changes. This suggests that SOS, LOS, and EOS are potentially useful for explaining NEE phenology over large landscapes.

The determination of NEE at large spatial scale and a large temporal scale is currently limited by the spatial coverage of flux tower sites, especially in the southern African region. Therefore, understanding the relationship between flux NEE phenology (CFP) and LSP derived from remotely sensed biophysical products would allow us to more accurately estimate NEE over large spatial extents. Such estimation would also allow for finer spatial resolution estimations of NEE complementary to products such as the Soil Moisture Active Passive Level 4 (SMAP L4) carbon product that is limited by its relatively course spatial resolution (9 km) (Jones et al., 2017).

The Fraction of Absorbed Photosynthetically Active Radiation (FAPAR) is a biophysical measure of photosynthetic activity. Although several FAPAR products are available, the MODIS fPAR and MISR-HR FAPAR products have the longest temporal coverage. Terra satellite's MODIS fPAR product is one of the longest and most consistent time series, available from the year 2000 at an 8-day repeat cycle and a 500 m spatial resolution. The single angle MODIS uses seven spectral bands and a land cover product for retrieval of vegetation FAPAR. However, Pinty *et al. (*2007) showed that the MODIS fPAR (hereon to be referred to as MODIS FAPAR) product also tends to have an analogous bias towards high FAPAR values. Therefore, in this study I also investigated the Multi-Angle imaging SpectroRadiometer High Resolution (MISR-HR) product that accounts for vegetation anisotropy as a possible alternative to MODIS (Verstraete et al., 2012).

Multi-angular observation significantly improves the estimation of vegetation structural parameters and hence MISR-HR has been shown to produce FAPAR that is far more consistent with in-situ FAPAR when compared to MODIS (Pinty et al., 2007). However, MISR-HR uses a Standard level 2 aerosol product at a spatial resolution of 17.6 km^2 to characterize atmospheric aerosols. When cloud cover is present, the product is considered as unreliable and a 17.6 km^2 region is skipped resulting in loss of data (Hu et al., 2006). Therefore, establishing which satellite-derived FAPAR product provides more consistent and ecologically accurate FAPAR information could be useful for future spatio-temporal studies of vegetation change and phenological patterns (Yan et al., 2016). An investigation of the relationship between FAPAR phenology from the two sensors and Net Ecosystem Exchange phenology could provide insight on how vegetation phenology patterns correlate to the carbon dynamics in the Kruger National Park.

This study analyzed the relationship between in-situ eddy covariance NEE measurements and satellite derived FAPAR phenology derived from MODIS and MISR-HR time series data, respectively. Furthermore, I determined the lag between remotely sensed FAPAR and in-situ CFP and assessed how closely the two satellite sensors' phenology matches CFP. Zhu et al. (2013) found that LSP can effectively reflect the spatial and temporal variations of CFP and therefore should be considered as a primary driver. Moreover, carbon sequestration tends to follow photosynthetic activity as well as leaf expansion (Balzarolo et al., 2016; Mendes et al 2020). I, therefore, expected that FAPAR time series would lead NEE time series, and that the start of season dates estimated by LSP would be earlier than those estimated from CFP. MISR-HR has been shown to have more accurate FAPAR values, and therefore I expected

that MISR-HR would have a closer relationship with in-situ NEE due to anisotropy than MODIS which tends to overestimate FAPAR (Gobron and Verstraete, 2009). I expected that the differences between LSP and CFP would not be significant, however that there would be a lag corresponding to the lag between FAPAR and NEE.

3.3 Methods

3.3.1 Study Area

The Kruger National Park (Figure 3.1) (22° 20'S to - 25° 32' S and 30° 47'E to 32° 00' E) is located on the north-eastern savanna region of South Africa and has a spatial extent of around two million hectares (Du Toit *et al.*, 2003). The park is characterized by a subtropical climate with hot mean summer temperatures (26.4 °C) and mild mean winter temperatures (9.5 °C) as well as seasonal variation in rainfall (Venter and Gertenbach, 1986). In the last five decades the mean minimum and mean maximum temperatures have increased by 0.8 °C (Venter and Gertenbach, 1986). Precipitation in the Kruger National Park follows a gradient whereby the south-western part receives an annual average of around 750 mm while the north eastern part receives 350 mm annual average (Venter and Gertenbach, 1986). The Skukuza flux tower is located on the south-western part of the Kruger National Park at 25.0197°S, 31.4969°E (Figure 3.1).

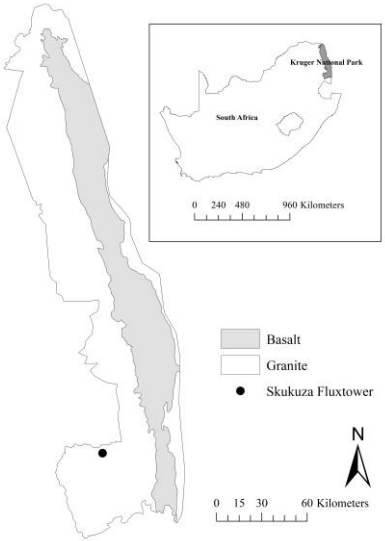


Figure 3.1: Illustrates the Kruger National Park (KNP) on the north-eastern part of South Africa. The Skukuza flux tower is located on the south-western part of the KNP in the granite geology.

3.3.2 MODIS fPAR and MISR-HR FAPAR

I used MODIS fPAR (MOD15A2H) data between 2001 and 2018. This data set has an 8-day time composite at 500 m spatial resolution and was acquired from the USGS Land Processes DAAC at EROS (http://mrtweb.cr.usgs.gov/). The MOD15A2H images were downloaded and re-projected from the MODIS sinusoidal projection to WGS84 UTM 36S in the MODIS conversion toolkit (MCTK) (White, 2019). I then extracted the fPAR and fPARLai_QC bands in ENVI IDL 8.5 (https://www.harrisgeospatial.com/Software-Technology/IDL). I subsetted and extracted the value of the central pixel (500 m) that falls over the geographic location of the Skukuza flux tower.

The MISR-HR FAPAR is derived from the Joint Research Center Two-stream Inversion Package (JRC-TIP). The JRC-TIP inversion process also delivers a cost function and estimate of variance associated with the FAPAR; the former is a measure of the distance between the model and the data, while the latter measures the uncertainty associated with the retrieved FAPAR (Clerici et al., 2010). To maximize temporal coverage of the FAPAR product I made use of all available Orbits of Block 110 for Path 168 and 169 that overlap the geographic location of the Skukuza flux tower. The overlapping area between these two Paths allowed for weekly observations over the study area, but staggered, i.e., 7 and 9 days. The path blocks covering the KNP area were all acquired in the local mode with a 385-km-wide swath and at 275 m spatial resolution. I then extracted the pixel corresponding to the geographic location over the Skukuza flux tower footprint in ENVI IDL 8.5. The TIP Cost Function model was used to cull less reliable FAPAR observations (Liu et al., 2018). The FAPAR values are derived from an inversion process and thus possess a level of accuracy and reliability which can be quantified with the cost function and the variance associated with the FAPAR values. When the cost function values of the FAPAR exceeded a threshold of 0.1 (i.e., the 90th percentile of its distribution) it was deemed unreliable and subsequently excluded, following the approach described in Liu et al. (2018). Higher cost function values represent a mismatch between the JRC-TIP model and input data. Discarding FAPAR observations associated with higher cost function values yields a time series of higher quality. The threshold value is guided by inspecting the histograms of the cost function distribution. The threshold of acceptability can be tailored to meet the specific needs of the user. The lower the threshold value, the higher the number of values culled, but the more reliable the inputs. The larger the threshold, the less the number of values culled, but the higher the number of observations included in the time series.

3.3.3 Eddy covariance data (EC)

Eddy covariance measurements of NEE flux from 2000 to present were used to derive in situ phenological metrics or CFP over a period of 18 years for the Skukuza flux tower location. NEE data is collected at 17 m aboveground which gives it a spatial coverage of approximately 500 m (Archibald *et al.,* 2009). I used a combination of two datasets to create the 18-year time series. The first dataset (2000 – 2014) was sourced from https://fluxnet.fluxdata.org/data/download-data/ and is part of the Tier 1 FLUXNET2015 dataset. The second dataset (2010 – 2018) was sourced from the Council for Scientific and Industrial Research (CISR) Pretoria, South Africa. Flux values were converted from hourly data to daily data by summing the hourly NEE values. Then NEE values were extracted based on the MODIS and MISR-HR acquisition dates for constructing the NEE time series. This resulted in two NEE time series', one matching MODIS acquisition dates and another matching MISR-HR acquisition dates. NEE values becoming negative, represents a point at which the system became a carbon sink (Archibald et al., 2009; McCombs et al., 2018). However, to make the interpretation of the analysis and interpretation of the relationship between carbon dynamics and the FAPAR phenology more intuitive, negative NEE values were changed to positive and vice versa.

3.3.4 Deriving phenology metrics

TIMESAT version 3.3 (Eklund and Jonsson, 2017) was used to reduce the time series noise and to derive phenology metrics from MODIS FAPAR, MISR-HR FAPAR and NEE. I thereby, performed curve fitting on the raw FAPAR and NEE data using the Savitzky Golay algorithm. This algorithm is robust and resistant to outliers (Eklund and Jonson, 2017). For the MISR-HR and MODIS data, I utilised weights determined through the TIP cost function and the QC (quality data) layer file, respectively. Further, to eliminate bias, I used a percentage of the seasonal amplitude to determine the start and end of season for both the FAPAR data and the NEE data. This method determines the start of season when the left part of the fitted curve reaches a fraction of the amplitude based on the user defined base level (Eklund and Jonsson, 2017). To determine these user-defined values for season start and end, I used the seasonal trend decomposition by Leoss (STL) method within TIMESAT. (Ekhlund and Jonsson, 2017; Wang et al., 2019). Accordingly, the Start of season was therefore specified at 30% of the seasonal amplitude and the End of season at 50% of the season amplitude.

FAPAR phenological metrics (Table 3.1) were generated from the fitted time series for the time period, 2001 to 2018. I specified the weights for the MODIS QC layer in TIMESAT as follows: values ranging from 0 - 7 were treated as good quality data and were given a weight of 1, and values ranging from 8 – 157 were a weight of 0.1. For MISR-HR data, values ranging from 1 – 1 (NaN values) were given a weight of 0.1, values ranging from 2 – 6 were given a weight of 0.5 and 7 – 12 (Good values) were given a weight of 1.

Table 3.1: Shows the abbreviations and notations used for the phenological metrics.

Phenological Metric	FAPAR (LSP)	NEE (CFP)
Start of Season	SOS	SOS_{NEE}
End of Season	EOS	EOS_{NEE}
Length of Season	LOS	CUP
Peak of Season	POS	POS_{NEE}

3.3.5 Data Analysis

I calculated the minimum, mean and maximum FAPAR values from the fitted time series over the study period to determine the differences in the FAPAR signal between MISR-HR and MODIS. Furthermore, I used the student's t-test to test for differences between the values of the two FAPAR time series'.

To study the relationship between MISR-HR FAPAR and flux NEE time series as well as MODIS FAPAR and flux NEE time series, I used a cross-correlation analysis on RStudio Desktop 1.3.1093 (https://rstudio.com/products/rstudio/release-notes/). Cross-correlation is a technique for comparing two time series that allows us to see how well one series predicts the values in the other (Dean and Dunsmuir 2016). As a prerequisite for cross-correlation (Dean and Dunsmuir 2016), I confirmed that the data was normally distributed using the Jarque-Bera test and that autocorrelation was constant using the Box-Pierce statistic.

A linear regression analysis was used to determine the relationship or association between phenological metrics derived using FAPAR (LSP) and flux NEE derived metrics (CFP). For most of the FAPAR data, there were 17 complete seasons that were determined in TIMESAT. However, NEE_{MISR}, there were only 16 seasons determined, whereby TIMESAT was characterizing two seasons as one long season over a two-year period. Furthermore, this NEE seasonality information extracted from TIMESAT could not detect two complete seasons (2005/06 and 2017/18) data due to low NEE values. I then used a nearest neighbour

technique to calculate the missing seasonality data. I confirmed normality of the data using the Shapiro-Wilk test. The parameters calculated were the Spearman's correlation coefficient (R^2), Root Mean Square Error (RMSE) and the significance statistic (p-value).

The student's t-test was then applied to determine if there were any statistically significant differences between actual phenological metrics/seasonality derived using MODIS FAPAR (LSP) and flux NEE (CFP) as well as between MISR-HR FAPAR and flux NEE. Using the Students's t-test, I also determined the mean signed difference for each phenology metric as denoted by Equation 3.1 (McCombs et al., 2018).

$$MSD = [(DOY_{FAPAR\ i} - DOY_{NEE,\ i}]/n \qquad \text{(Equation 3.1)}$$

3.4 Results

3.4.1 Time series comparison between FAPAR and NEE

The comparison between the minimum, mean, and maximum values of the two FAPAR time series indicated that there were indeed significant differences (t-test: t=-14.90, d.f = 1570, $p<0.001$). The MISR-HR sensor had an average FAPAR value of 0.30 while MODIS had an average of 0.41. The sensors also had a different range of FAPAR values whereby MISR-HR ranged from 0.05 to 0.60 while MODIS ranged from 0.10 to 0.77. Both sensors recorded below average values of FAPAR for the year 2016. NEE followed similar trends to both MISR-HR and MODIS FAPAR time series and showed a very low response for 2016 as well as 2007. NEE showed intra-annual variation in seasonality sometimes showing dual seasonality especially in the 2010/11 season whereby the NEE changes from being a sink to a source twice (Figure 3.2). A lag was apparent as from 2009 onwards between the MISR-HR and MODIS.

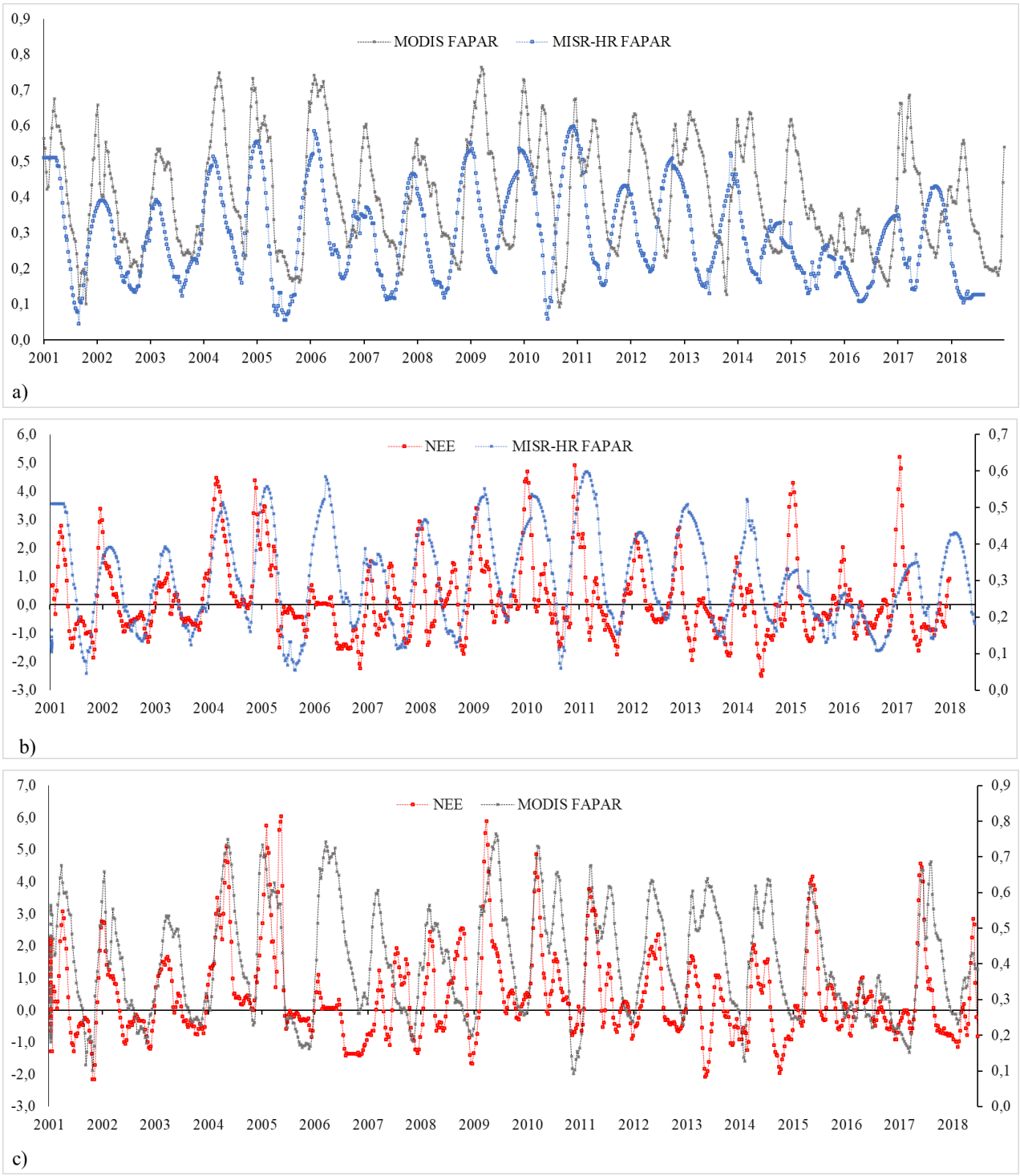


Figure 3.2: A comparison between a) MISR-HR and MODIS FAPAR, b) MISR-HR FAPAR and flux NEE and c) MODIS and flux NEE all fitted using the Savitzky Golay model at the Skukuza flux tower site, Kruger National Park.

3.4.2 Cross-correlation Analysis

There were significant positive correlations between FAPAR and flux NEE from -5 composites lag to 15 composites lag (Figure 3.3a and 3.3b). However, the highest and strongest correlation was at lag 1 indicating an 8-day lag between MODIS FAPAR and NEE throughout the study period (Figure 3.3a). This suggests that NEE shows a trend/response 8 days after a change in FAPAR. There were also significant positive correlations between MISR-HR FAPAR and NEE, however the strongest correlation was at a longer lag than MODIS (3 composites = 23 days) (Figure 3.3b). Negative correlations were also apparent around lag -17 and lag 26, suggesting a period lag in which high FAPAR values are associated with very low NEE values (Figure 3.3a and 3.3b).

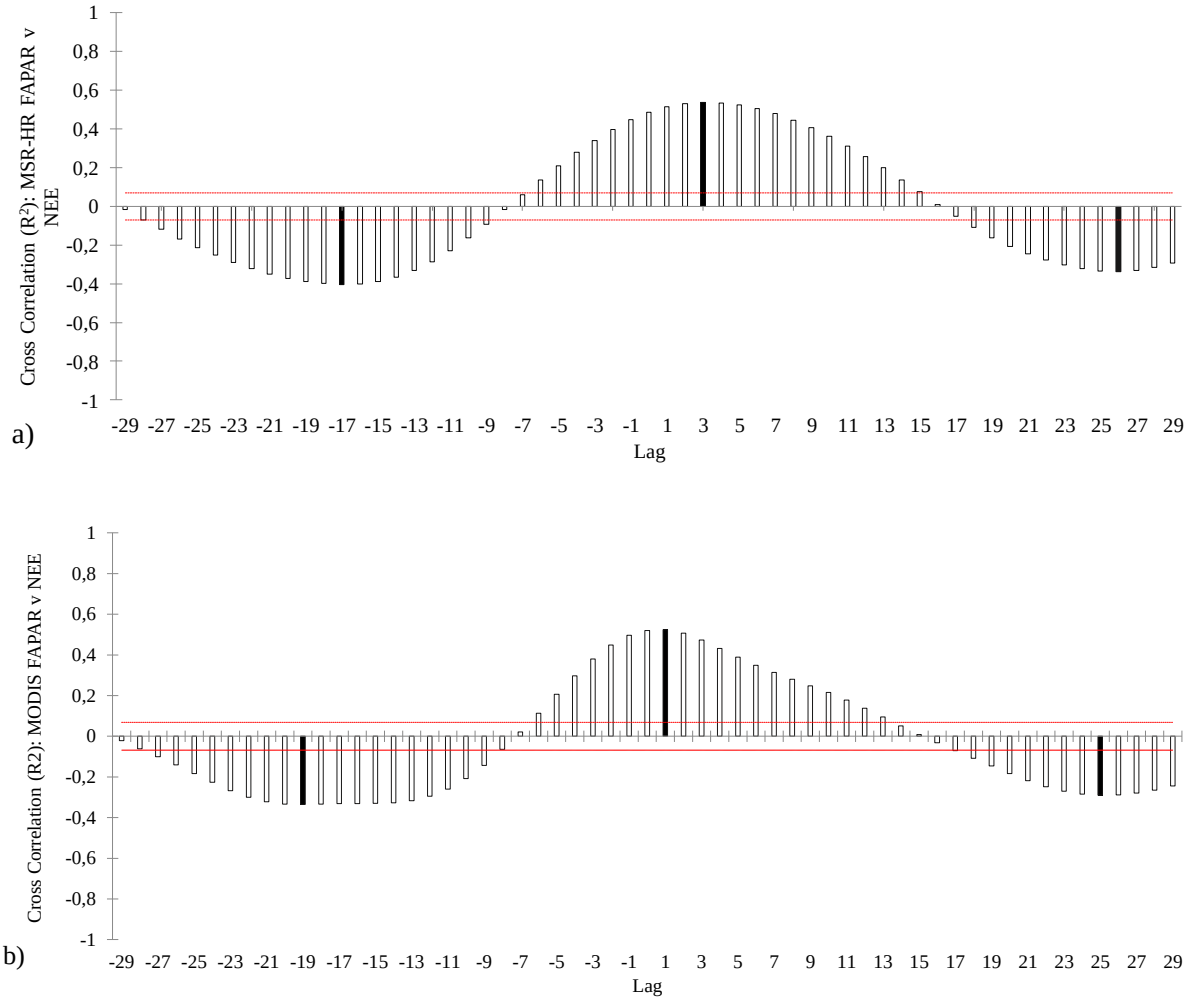


Figure 3.3: Cross-correlation between a) MISR-HR and NEE and b) MODIS and NEE. A single lag unit corresponds to 8-days for MODIS and 9/7 days for MISR-HR and corresponding NEE. The shaded bars show the highest correlation coefficient and the red horizontal represents the 95% confidence intervals.

3.4.3 Relationship between Carbon flux phenology and FAPAR derived phenology.

There were statistically significant positive relationships between SOS_{FAPAR} from both sensors and SOS_{NEE} (Figure 3.4). $SOS_{MISR-HR}$ had a stronger association to the SOS_{NEE} (R^2 = 0.6) (Figure 3.4a) compared to SOS_{MODIS} (R^2 = 0.28) (Figure 3.4b). In addition, MISR-HR showed a smaller Root Mean Square Error (RMSE) (20 days) when compared to MODIS (23 days). Beside the SOS, there were no other statistically significant relationships between the metrics derived from FAPAR and NEE flux for the study period (Table 3.2).

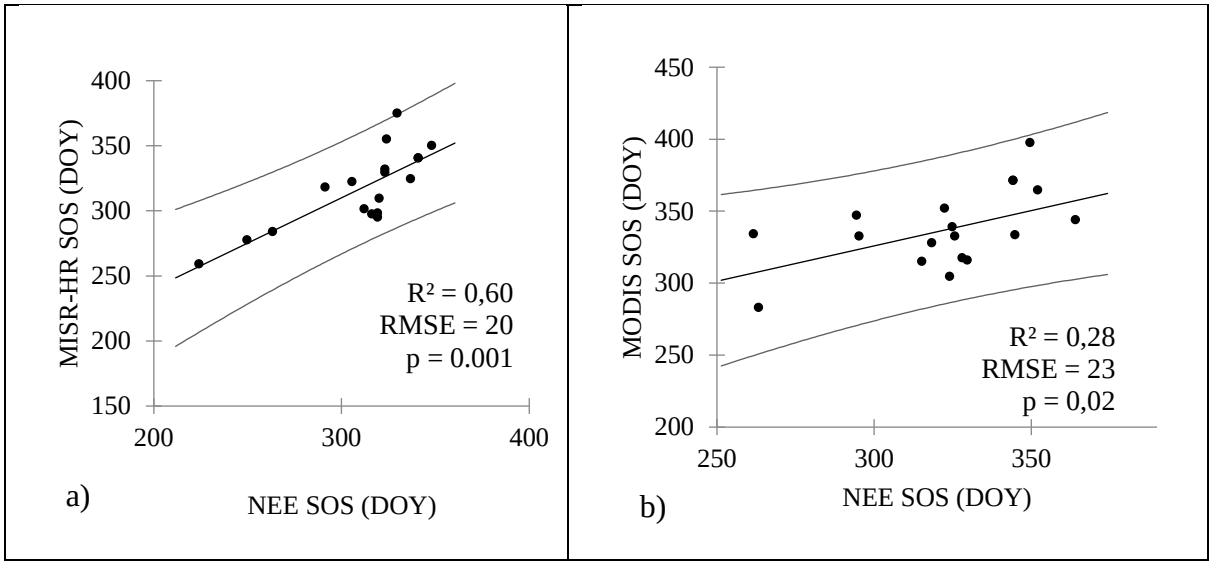


Figure 3.4: The relationship between a) SOS_{NEE} and $SOS_{MISR-HR}$ and b) SOS_{NEE} and SOS_{MODIS} in the Skukuza flux tower, Kruger National Park.

Table 3.2: Showing the relationships between carbon flux phenology and FAPAR phenology. NEE metrics (SOS_{NEE}, EOS_{NEE}, CUP, and POS_{NEE}) were correlated to corresponding MISR and MODIS LSP metrics.

	EOS_{MODIS}/ EOS_{NEE}	$EOS_{MISR-HR}$/ EOS_{NEE}	POS_{MODIS}/ POS_{NEE}	$POS_{MISR-HR}$/ POS_{NEE}	LOS_{MODIS}/ CUP	$LOS_{MISR-HR}$/ CUP
R^2	**0,01**	**0,01**	**0,01**	**0,12**	**0,02**	**0,08**
RMSE	70,4	20,5	32,0	25,6	40,4	33,3
p	**0,74**	**0,67**	**0,76**	**0,17**	**0,56**	**0,27**

3.4.3 Timing differences between CFP and LSP metrics.

There were only 2 statistically significant differences between CFP and LSP (EOS_{MODIS} and $POS_{MISR-HR}$). The results also show that the differences in the phenometrics vary season to season by up to 5.11 composites (~41 days) (Table 3.3). The smallest differences were between $EOS_{MISR-HR}$ and EOS_{NEE} with an MSD of 0.91 composites (~7 days) and $SOS_{MISR-HR}$ and SOS_{NEE} with an MSD of 1.14 composites (~9 days). These result show that $MISR_{FAPAR}$ season starts approximately 9 days before the NEE_{SOS} while the MODIS season tends to start about 15 days before NEE_{SOS}.

Table 3.3: The differences in SOS, EOS, and POS between FAPAR derived from MODIS and MISR-HR and NEE (1 MODIS composite = 8 days; 1 MISR-HR composite 7/9 days)

	MODIS SOS	MISR-HR SOS	MODIS EOS	MISR-HR EOS	MODIS CUP	MISR-HR CUP	MODIS POS	MISR-HR POS
Difference	1,90	1,14	-4,97	0,91	3,06	1,25	1,86	5,11
t	1,60	0,84	-2,19	0,52	1,28	0,51	1,10	4,06
|t|	2,04	2,04	2,04	2,04	2,04	2,04	2,04	2,04
DF	32	32	32	32	32	32	32	32
p-value	0,120	0,408	0,036	0,608	0,209	0,612	0,281	0,000

.5 Discussion

Savanna phenology and its relationship with carbon dynamics in the Kruger National Park is still largely understudied. This study therefore assessed the relationship between in-situ eddy covariance Net Ecosystem Exchange measurements and satellite derived FAPAR time series as well as phenology metrics from MODIS and MISR-HR (land surface phenology), and phenology from NEE measurements (carbon flux phenology) respectively.

To understand the respective relationships of land surface phenology to NEE, it is important to understand the inherent differences of the two sensors. Firstly, MODIS tends to overestimate FAPAR when in situ observations are under 0.6 (Fensholt et al., 2004; Zhang et al., 2014; Chernetskiy et al., 2017). My results indicated that MODIS does have a bias towards higher FAPAR values when compared to MISR-HR. On the contrary, JRC-TIP

derived MISR-HR product has been shown to only underestimate FAPAR when in situ FAPAR is over 0.8 and is therefore more closely related to in situ FAPAR (Chernetskiy et al., 2017). Such underestimation of FAPAR by MISR-HR is however only caused by interpolation of sparse data points due to large numbers of missing data (Chernetskiy et al. 2017). Despite the large number of missing values for the MISR-HR data in my study, there was a strong relationship between MISR-HR FAPAR and in situ NEE indicating that the Savitzky Golay fitting algorithm is an effective model for gap filling the MISR-HR data.

Cross-correlation analyses showed that remotely sensed FAPAR time series' from MODIS and MISR-HR have a significant relationship with in-situ NEE however, both satellite products showed that there is a lag between FAPAR and NEE whereby changes in FAPAR lead to a NEE response several days later. Flux NEE represents both aboveground plant respiration as well as soil respiration. In fact, Archibald et al. (2009) showed that the maximum CO_2 uptake occurs at low levels of soil moisture albeit while leaves are still green, since in these conditions the contribution of soil respiration is low. On the other hand, the maximum FAPAR or gross primary productivity tended to occur a few days after an increase in soil moisture (Archibald et al., 2009). Therefore, the lags could be caused by the opposing effects that soil moisture has on FAPAR and NEE combined with contributions of soil respiration to NEE (Luo and Zhuo, 2006). Moreover, gross primary productivity and net ecosystem exchange tend to follow after leaf expansion where the photosynthetic activity becomes high (Luo and Zhu, 2006). This could be why FAPAR leads the NEE especially when it comes to the start of season metric. Unexpectedly, MODIS time series showed a closer relationship with in-situ NEE than MISR-HR time series with only a lag of 8 days. MISR-HR displayed a 23-day lag between the smoothed FAPAR and NEE time series' despite the missing data.

SOS_{FAPAR} had the closest association with in-situ SOS_{NEE}, similar to studies in four different North American biomes (Zhu et al., 2013) and in woody savannas, deciduous and broadleaf forest sites (Gonsamo et a., 2012; Balzarolo et al.,2015). My results did not agree with other studies that state that LOS_{NEE} correlates to the length of the growing season (Archibald et al., 2009; Zhu et al., 2013; McCombs et al., 2018). However, it is important to note that NEE showed a large amount of intra-seasonal variability in years such as 2006/7 and almost displaying dual seasonality in 2013/14. For instance, in the years 2010 and 2011, the NEE changes from being a sink to a source twice in each year. However, during those two years, TIMESAT would estimate two distinct seasons for FAPAR, but would estimate one long

season for NEE. This may have been caused by of the gap-filling of missing data in the eddy covariance data set (Nickless et al., 2011). This caused inaccuracies in the estimated date of EOS_{NEE} and EOS_{LOS}. Indeed, SOS_{NEE} estimation is generally better than EOS_{NEE} estimation due to complications between canopy-structure based phenology metrics and carbon fluxes (Garrity et al., 2011; Zhu et al., 2013; McCombs et al., 2018). Therefore, the lack of a relationship between LOS and LOS_{NEE}, and between EOS and EOS_{NEE} could be ascribed to less accurate estimation of these metrics. Interestingly, however, MISR-HR SOS showed a stronger association with SOS_{NEE} when compared to MODIS. This suggested that SOS derived from MISR-HR FAPAR could be more suitable than SOS derived from MODIS FAPAR for predicting the SOS_{NEE} for the Kruger National Park and or the savanna region.

The only two significant Mean Signed Differences (MSD's) between LSP and CFP were in EOS_{MODIS} and the $POS_{MISR\text{-}HR}$. The MSDs were consistent with the cross-correlation results which showed that FAPAR changes a few days before NEE, with differing inter-seasonal magnitudes. MISR-HR derived phenology showed the least difference in SOS, EOS and LOS when compared to CFP. While my study was done in a heterogenous flux site consisting of both tree and grass phenology, my results were consistent with McCombs et al. (2018) who found an MSD of around 9 days between SOS and SOS_{NEE} and about 7 days between EOS and EOS_{NEE}. The results of my study therefore suggest that MISR-HR could accurately estimate SOS_{NEE} within 0-8 days. Most of the MISR-HR data points were determined using interpolation, and therefore did not accurately indicate the peak of season as well as the finer relationship with NEE. MODIS FAPAR time series were on the other hand more temporally consistent and the POS was therefore more accurately defined. However, overestimation of FAPAR by MODIS resulted in larger differences between LSP and CFP.

In conclusion, this study showed that there is a strong relationship between FAPAR and NEE albeit with a lag of at least 8 days. I also showed that MISR-HR performs better at explaining the start of carbon uptake and could be useful for future carbon studies. Furthermore, I found that the LSP does not differ significantly from CFP . While MISR-HR FAPAR phenology metrics showed a much closer relationship with in-situ NEE phenology metrics derived from the flux tower measurements, there are still some limitations towards modelling carbon flux using FAPAR. Firstly, remote sensing data represents an instantaneous snapshot of the radiation reflected from the top of canopy, while flux towers record dynamic changes throughout the day. The second limitation is in accurately estimating the CFP metrics in a way that accounts for intra-seasonal variability caused by disturbances such as fire. Thirdly,

the MISR-HR dataset was rife with missing data. For future studies that aim to study the relationship between FAPAR and NEE, I suggest that a model for determining CFP should take into account the effects of disturbances on NEE and FAPAR. To address the shortcomings of both sensors, future studies could explore a harmonized FAPAR time series of both MODIS and MISR-HR FAPAR. Furthermore, it should incorporate optimal data on climate variables or estimating CFP dates as it drastically improves the results as shown by Zhu et al. (2013).

3.6 References

Archibald, S. A., Kirton, A., van der Merwe, M. R., Scholes, R. J., Williams, C. A., and Hanan, N. 2009. Drivers of inter-annual variability in net ecosystem exchange in a semi-arid savanna ecosystem, South Africa. *Biogeosciences*, 6, pp. 251–266.

Balzarolo, M., Vicca, S., Nguy-Robertson, A.L., Bonal, D., Elbers, J.A., Fu, Y.H., Grünwald, T., Horemans, J.A., Papale, D., Peñuelas, J. and Suyker, A., 2016. Matching the phenology of net ecosystem exchange and vegetation indices estimated with MODIS and FLUXNET in-situ observations. *Remote Sensing of Environment*, *174*, pp.290-300.

Chernetskiy, M., Gómez-Dans, J., Gobron, N., Morgan, O., Lewis, P., Truckenbrodt, S. and Schmullius, C., 2017. Estimation of FAPAR over croplands using MISR data and the earth observation land data assimilation system (EO-LDAS). *Remote Sensing*, *9*(7), p.656.

Clerici, M.; Vossbeck, M.; Pinty, B.; Kaminski, T.; Taberner, M.; Lavergne, T.; Andredakis, I. Consolidating the Two-Stream Inversion Package (JRC-TIP) to Retrieve Land Surface Parameters from Albedo Products. IEEE J. Sel. Top. Appl. Earth Obs. Remote Sens. 2010, 3, 286–295.

Chuine, I., 2010. Why does phenology drive species distribution? *Philosophical Transactions of the Royal Society B: Biological Sciences*, *365*(1555), pp.3149-3160.

Dean, R.T. and Dunsmuir, W.T., 2016. Dangers and uses of cross-correlation in analyzing time series in perception, performance, movement, and neuroscience: The importance of constructing transfer function autoregressive models. *Behavior research methods*, *48*(2), pp.783-802.

Eklundh, L. and Jönsson, P. 2012. *Timesat 3.1 Software Manual*. Lund University, Sweden.

Eklundh, L. and Jönsson, P.T., 2017. 3.3 with Seasonal Trend Decomposition and Parallel Processing—Software Manual. *Lund University: Lund, Sweden*, p.88.

Fensholt, R., Sandholt, I. and Rasmussen, M.S., 2004. Evaluation of MODIS LAI, fAPAR and the relation between fAPAR and NDVI in a semi-arid environment using in situ measurements. *Remote Sensing of Environment*, *91*(3-4), pp.490-507.

Garrity, S.R., Bohrer, G., Maurer, K.D., Mueller, K.L., Vogel, C.S. and Curtis, P.S., 2011. A comparison of multiple phenology data sources for estimating seasonal transitions in deciduous forest carbon exchange. *Agricultural and Forest Meteorology*, *151*(12), pp.1741-1752.

Gessner, U., Knauer, K., Kuenzer, C. and Dech, S., 2015. Land surface phenology in a West African Savanna: impact of land use, land cover and fire. In *Remote Sensing Time Series* (pp. 203-223). Springer, Cham.

Gonsamo, A., Chen, J.M., Wu, C. and Dragoni, D., 2012. Predicting deciduous forest carbon uptake phenology by upscaling FLUXNET measurements using remote sensing data. *Agricultural and Forest Meteorology*, *165*, pp.127-135.

Gobron, N. and Verstraete, M., 2009. Ecv T10: fraction of absorbed photosynthetically active radiation (FAPAR). *Essential Climate Variables*, p.23.

Jolly, W. M., and Running, S. W. (2004). Effects of precipitation and soil water potential on drought deciduous phenology in the Kalahari. *Global Change Biology*, 10, pp. 303–308.

Jones, L.A., Kimball, J.S., Reichle, R.H., Madani, N., Glassy, J., Ardizzone, J.V., Colliander, A., Cleverly, J., Desai, A.R., Eamus, D. and Euskirchen, E.S., 2017. The SMAP Level 4 Carbon Product for Monitoring Ecosystem Land–Atmosphere CO 2 Exchange. *IEEE Transactions on Geoscience and Remote Sensing*, *55*(11), pp.6517-6532.

Liu, Z., Verstraete, M.M. and de Jager, G., 2018. Handling outliers in model inversion studies: a remote sensing case study using MISR-HR data in South Africa. *South African Geographical Journal*, *100*(1), pp.122-139.

McCombs, A.G., Hiscox, A.L., Wang, C., Desai, A.R., Suyker, A.E. and Biraud, S.C., 2018. Carbon flux phenology from the sky: Evaluation for maize and soybean. *Journal of Atmospheric and Oceanic Technology*, *35*(4), pp.877-892.

Mendes, K.R., Campos, S., da Silva, L.L., Mutti, P.R., Ferreira, R.R., Medeiros, S.S., Perez-Marin, A.M., Marques, T.V., Ramos, T.M., de Lima Vieira, M.M. and Oliveira, C.P., 2020. Seasonal variation in net ecosystem CO 2 exchange of a Brazilian seasonally dry tropical forest. *Scientific Reports*, *10*(1), pp.1-16.

Pinty, B., Lavergne, T., Voßbeck, M., Kaminski, T., Aussedat, O., Giering, R., Gobron, N., Taberner, M., Verstraete, M.M. and Widlowski, J.L., 2007. Retrieving surface parameters for climate models from Moderate Resolution Imaging Spectroradiometer (MODIS)-Multiangle Imaging Spectroradiometer (MISR) albedo products. *Journal of Geophysical Research: Atmospheres*, *112*(D10).

Van Wilgen, N.J., Goodall, V., Holness, S., Chown, S.L. and McGeoch, M.A., 2016. Rising temperatures and changing rainfall patterns in South Africa's national parks. *International Journal of Climatology*, *36*(2), pp.706-721.

Venter, F.J. and Gertenbach, W.P.D., 1986. A cursory review of the climate and vegetation of the Kruger National Park. *Koedoe*, *29*(1), pp.139-148.

Verma, M., Friedl, M.A., Richardson, A.D., Kiely, G., Cescatti, A., Law, B.E., Wohlfahrt, G., Gielen, B., Roupsard, O., Moors, E.J. and Toscano, P., 2014. Remote sensing of annual terrestrial gross primary productivity from MODIS: an assessment using the FLUXNET La Thuile data set. *Biogeosciences*, *11*(8), p.2185.

Yan, K., Park, T., Yan, G., Liu, Z., Yang, B., Chen, C., ... & Myneni, R. B. (2016). Evaluation of MODIS LAI/FPAR product collection 6. Part 2: Validation and intercomparison. Remote Sensing, 8(6), 460.

Zhang, Q., Cheng, Y.B., Lyapustin, A.I., Wang, Y., Gao, F., Suyker, A., Verma, S. and Middleton, E.M., 2014. Estimation of crop gross primary production (GPP): fAPARchl versus MOD15A2 FPAR. *Remote Sensing of Environment*, *153*, pp.1-6.

Zhu, W., Chen, G., Jiang, N., Liu, J. and Mou, M., 2013. Estimating carbon flux phenology with satellite-derived land surface phenology and climate drivers for different biomes: A synthesis of AmeriFlux observations. *PloS one*, *8*(12), p.e84990.

Chapter 4

4. Discussion and Synthesis

Natural systems such as National Parks are primarily managed to maintain and preserve biodiversity. The financial resources to accomplish this are usually gained through tourism and sponsorship (Yessoufou, 2017). Tourism is vulnerable to disruption by extreme weather events and hazardous events, such as fires, floods, droughts, as well as global pandemics (Rogerson and Rogerson, 2020). For instance, the South African tourism industry has recently been devastated by the Covid 19 pandemic due to international and local travel restrictions (Rogerson and Rogerson, 2020). This, along with other factors means that financial resources are not always available for the management of such natural systems especially in Africa (SANParks, 2008; Yessoufou, 2017).

There has been an increase in evidence that natural systems are important carbon reservoirs and tend to store a larger quantity of carbon than monoculture plantations (Marchetti et al., 2012; Yessoufou, 2017). Therefore, the economic valuation of the carbon reservoir could provide a sustainable financial source for the management of these natural systems through numerous carbon initiatives (Yessoufou, 2017). The study of the carbon reservoir as well as carbon flux phenology in the southern African region is limited by the sparse spatial coverage of flux tower sites and the high costs associated with field-based monitoring. Therefore, establishing the relationship between NEE phenology and remotely sensed land surface phenology could lead to an improvement of NEE estimates over the entire landscape using remote sensing products. Additionally, it could allow for continuous monitoring that is a requirement of carbon initiatives such as the United Nations reducing emissions from deforestation and forest degradation (REDD+). Furthermore, recent studies have shown that encroachment reduces the carbon stock in South Africa, and this reduces the amount of carbon emissions that can be offset. This is particularly important when considering carbon sequestration as an ecosystem service and as a commodity to and devising methods for carbon accounting (Stafford et al., 2017). But there is limited knowledge on how changes in vegetation distribution relates to changes in the carbon stock. Yessoufou (2017) showed that ecological heterogeneity of the Park remains one of the biggest limitations in quantifying the carbon reservoir. Therefore, given the spatial heterogeneity of the Kruger National Park it was important that we established how the phenology of the different landscapes that have

contrasting climates and consist of varied geology types are responding to change. The aim of this study was therefore to firstly, describe landscape-scale phenology trends across different regions within the KNP and secondly to investigate how land surface phenology trends relate to carbon flux phenology using the Skukuza flux tower site as a study site.

One particularly crucial change trend was the localized decline in the length of growing season across the KNP. Archibald et al., 2009 stressed how important the presence of green leaves is to Net Ecosystem Exchange (NEE) and generally the amount of biomass that can store carbon. Although the intra-seasonal variability of NEE was a huge limitation in describing the relationship between LOS_{NEE} and LOS_{FAPAR} in TIMESAT, the relationship between the SOS_{NEE} and SOS_{FAPAR} did indicate that NEE follows FAPAR. This is further corroborated by the strong relationship between FAPAR and NEE shown by the cross-correlation analysis in my study. Hence, the decrease in length of season shown by the pixel level analysis in my second chapter, means that the overall time in which vegetation is photosynthetically active is decreasing over time and the amount of time in which the system is a sink could also decrease if the trend remains. Similarly, the overall loss of biomass shown by the declining large integral could potentially result in less carbon being stored in the landscape should these trends remain (Archibald et al., 2009).

As mentioned in chapter 3, the behaviour of the NEE time series was similar to that of the MODIS time series, especially in years such as 2016 (drought year) where FAPAR and NEE both had very low values. This may suggest that soil moisture availability is a crucial factor here for both gross primary productivity and carbon sequestration. Additionally, the localized decreases in accumulated biomass in the southern region could be indicative of the impact of extreme droughts on the loss of woody vegetation over time and further reduce the amount of sequestered aboveground carbon. However, projections by Bunting et al. (2016) show that the drought tolerant Mopane that is currently dominant in the northern bioregion of the park could offset the loss of vegetation in the southern region in the long term. This suggests that there would be shifts in vegetation distribution as well as abundance in the Kruger National Park over the next decade. However, the extent to which this would affect the carbon stock of the KNP is unknown since there are no records showing the contribution of the different vegetation functional types/communities to the carbon stock.

Another objective of this study was, to assess the potential utility of two moderate resolution satellite sensors for estimating in-situ phenology and estimating carbon dynamics over a

long-term period. The pixel level regression showed much promise here, especially because it characterizes seasonality changes at a spatial resolution of 500 m. Although I could not assess the accuracy or validate the change trends of LSP based on ground phenology data due to limitations in the continuity and consistency of ground observations in the KNP, Eddy covariance flux data did provide a suitable alternative for verifying land surface phenology. The strong relationship between NEE and FAPAR firstly indicated that at moderate resolution, remote sensing is a valid methodology for estimating carbon dynamics and in-situ phenology and perhaps could be a useful proxy for NEE where flux data is unavailable. However, due to the heterogeneity of the Kruger National Park, additional long-term carbon flux measurements are required to construct valid models for estimating NEE throughout the park, especially because long term carbon flux data is currently limited to only two flux towers which only represents only 500 m of two million hectares each. Moreover, there are no long-term records of phenology in the in the region to supplement this data. The expansion of the flux tower network combined with phenocams would help us to understand the carbon dynamics and more importantly how carbon flux trends in relation to changes in vegetation distribution and phenology.

Understanding carbon dynamics is essential for climate change mitigation and adaptation in protected areas such as the KNP. With limited research infrastructure and funding in southern Africa to monitor in situ vegetation dynamics and associated ecosystem functional changes, it is imperative to establish methods by which we can estimate and predict past and future changes at the landscape scale. Additionally, it is important for continuous monitoring and accurate modelling of the carbon reservoir and flux required by carbon initiatives (Yessoufou, 2017). My study was a foundation for using remote sensing for understanding phenology and its relationship with the carbon cycle in the KNP. I found that given the strong relationship between LSP and CFP, the period of carbon sequestration might decrease in the KNP due to the loss of woody vegetation in the southern region. Moreover, I found that moderate resolution sensor FAPAR provides a suitable proxy for NEE. However, there were a few limitations to my study. Future studies should aim at establishing a method for determining the end of carbon uptake and peak of carbon uptake that accounts for limitation caused by the robustness and intra-seasonal variability of NEE. Moreover, rainfall should be analyzed at a much finer spatial scale and incorporated into the model for estimating the phenological metrics. Future studies could also compare pixel level phenology derived from

MODIS/MISR-HR with pixel-based carbon products such as the SMAP L4 to establish the spatio-temporal relationships between FAPAR and carbon.

4.1 References

Archer, E.R., Engelbrecht, F.A., Hänsler, A., Landman, W., Tadross, M. and Helmschrot, J., 2018. Seasonal prediction and regional climate projections for southern Africa. In *Climate change and adaptive land management in southern Africa – assessments, changes, challenges, and solutions,* pp. 14-21 Klaus Hess Publishers.

Archibald, S. A., Kirton, A., van der Merwe, M. R., Scholes, R. J., Williams, C. A., and Hanan, N. 2009. Drivers of inter-annual variability in net ecosystem exchange in a semi-arid savanna ecosystem, South Africa. *Biogeosciences*, 6, pp. 251–266.

Liang, L. and Schwartz, M.D., 2009. Landscape phenology: an integrative approach to seasonal vegetation dynamics. *Landscape Ecology*, *24*(4), pp.465-472.

Masia, N.D., Stevens, N. and Archibald, S., 2018. Identifying phenological functional types in savanna trees. *African Journal of Range and Forage Science*, *35*(2), pp.81-88.

Rogerson, C.M. and Rogerson, J.M., 2020. COVID-19 Tourism impacts in South Africa: Government and industry responses. *Geo Journal of Tourism and Geosites*, *31*(3), pp.1083-1091.

Stafford, W., Birch, C., Etter, H., Blanchard, R., Mudavanhu, S., Angelstam, P., Blignaut, J., Ferreira, L. and Marais, C., 2017. The economics of landscape restoration: Benefits of controlling bush encroachment and invasive plant species in South Africa and Namibia. *Ecosystem Services*, *27*, pp.193-202.

Whitecross, M.A., Witkowski, E.T.F. and Archibald, S., 2016. No two are the same: Assessing variability in broad-leaved savanna tree phenology, with watering, from 2012 to 2014 at Nylsvley, South Africa. *South African Journal of Botany*, *105*, pp.123-132.

Whitecross, M.A., Witkowski, E.T.F. and Archibald, S., 2017. Savanna tree-grass interactions: A phenological investigation of green-up in relation to water availability over three seasons. *South African Journal of Botany*, *108*, pp.29-40.

Yessoufou, K., 2017. Potential carbon stock in the Kruger National Park, South Africa. *Botany Letters*, *164*(4), pp.425-432.

Zhu, W., Chen, G., Jiang, N., Liu, J. and Mou, M., 2013. Estimating carbon flux phenology with satellite-derived land surface phenology and climate drivers for different biomes: A synthesis of AmeriFlux observations. *PloS one*, *8*(12), p.e84990.

5. Appendix

Table 1.1: Shows the criteria used to interpret the QC layer file from MODIS. For instance, integer values ranging from 0 – 7 represented good quality data, quality detection, no cloud cover, and no saturation as per the MODIS interpretation guide.

Integer_ Value	Bit 7	Bit 6	Bit 5	Bit 4	Bit 3	Bit 2	Bit 1	Bit 0	Sensor Quality	Sensor	Quality Detectors	Cloud Cover	Saturation
0	0	0	0	0	0	0	0	0	Good Quality	Terra	Good Quality detectors	0: No Significant Clouds	Main RT: Best result (No saturation)
1	0	0	0	0	0	0	0	1	Other Quality	Terra	Good Quality detectors	0: No Significant Clouds	Main RT: Best result (No saturation)
2	0	0	0	0	0	0	1	0	Good Quality	Aqua	Good Quality detectors	0: No Significant Clouds	Main RT: Best result (No saturation)
3	0	0	0	0	0	0	1	1	Other Quality	Aqua	Good Quality detectors	0: No Significant Clouds	Main RT: Best result (No saturation)
4	0	0	0	0	0	1	0	0	Good Quality	Terra	Good Quality detectors	0: No Significant Clouds	Main RT: Best result (No saturation)
5	0	0	0	0	0	1	0	1	Other Quality	Terra	Good Quality detectors	0: No Significant Clouds	Main RT: Best result (No saturation)
6	0	0	0	0	0	1	1	0	Good Quality	Aqua	Good Quality detectors	0: No Significant Clouds	Main RT: Best result (No saturation)
7	0	0	0	0	0	1	1	1	Other Quality	Aqua	Good Quality detectors	0: No Significant Clouds	Main RT: Best result (No saturation)
8	0	0	0	0	1	0	0	0	Good Quality	Terra	Bad Detectors	1: Significant Clouds	Main RT: Best result (No saturation)
9	0	0	0	0	1	0	0	1	Other Quality	Terra	Bad Detectors	1: Significant Clouds	Main RT: Best result (No saturation)
10	0	0	0	0	1	0	1	0	Good Quality	Aqua	Bad Detectors	1: Significant Clouds	Main RT: Best result (No saturation)

Table 1.2: Timeseries normality and white noise tests for MODIS FAPAR/ NEE

Statistic	DF	Value	p-value
Box-Pierce	6	157,389	< 0,0001
Ljung-Box	6	158,680	< 0,0001
McLeod-Li	6	2223,279	< 0,0001
Box-Pierce	12	686,143	< 0,0001
Ljung-Box	12	694,928	< 0,0001
McLeod-Li	12	2696,121	< 0,0001

Table 1.3: Timeseries normality and white noise tests for MISR-HR FAPAR/ NEE

Statistic	DF	Value	p-value
Box-Pierce	6	183,433	< 0,0001
Ljung-Box	6	185,042	< 0,0001
McLeod-Li	6	1303,839	< 0,0001
Box-Pierce	12	823,308	< 0,0001
Ljung-Box	12	834,874	< 0,0001
McLeod-Li	12	2472,861	< 0,0001

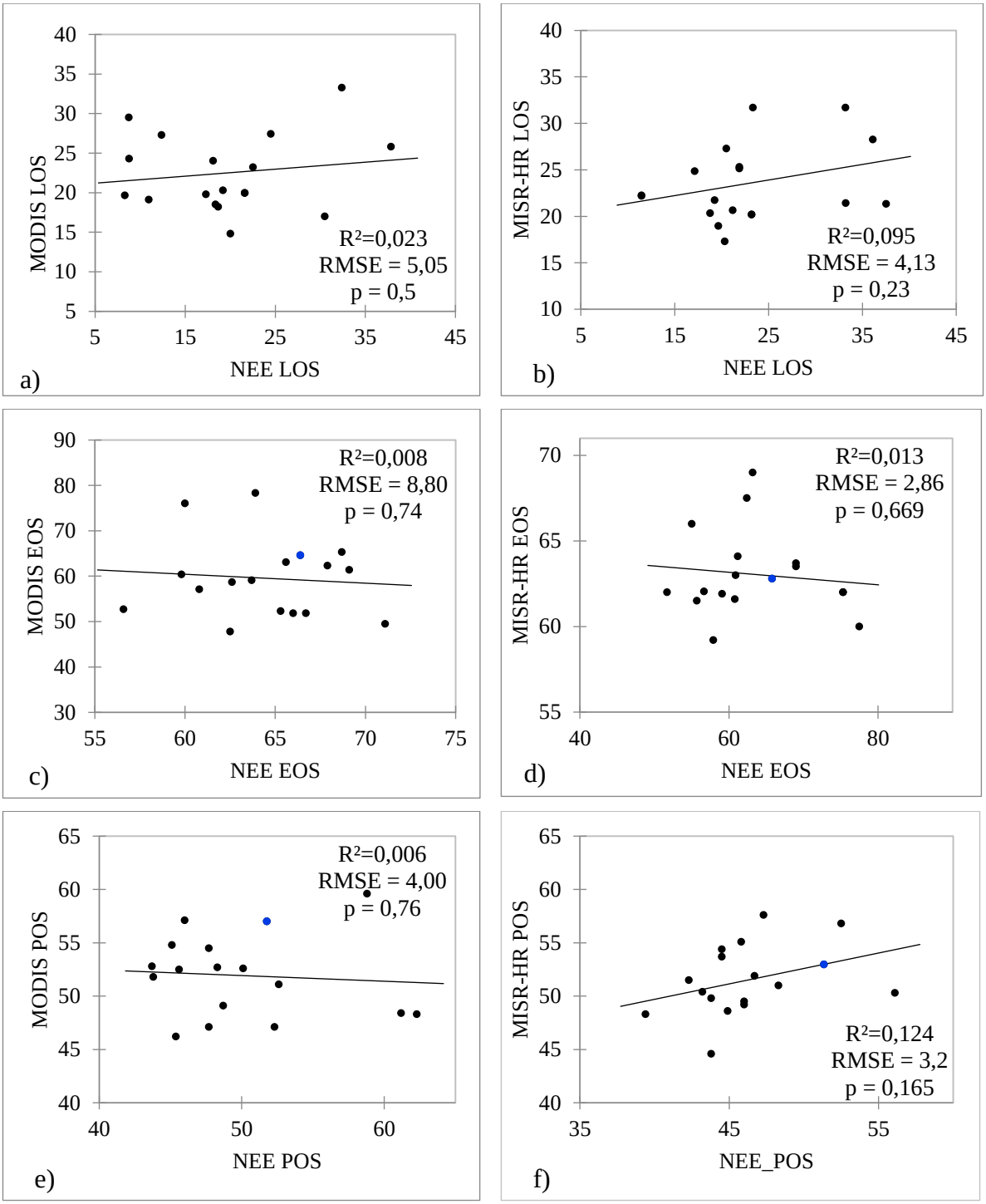


Figure 3.1: The relationship between LSP and CFP derived from MODIS, MISR-HR and NEE at the Skukuza flux tower, Kruger National Park.

Table 1.3: MODIS and NEE derived SOS seasonality at the skukuza flux tower.

Season	MODIS SOS	NEE SOS
1	41,02	39,79
2	46,44	43,02
3	49,7	43,7
4	39,5	41,2
5	42,4	40,6
6	43	45,5
7	38,1	40,5
8	41,7	43,1
9	41,6	40,7
10	39,4	39,4
11	44	40,3
12	35,4	32,9
13	39,7	41
14	41,8	32,7
15	41,6	36,9
16	45,6	44
17	43,4	36,8

Table 1.4: MISR-HR and NEE derived SOS seasonality at the skukuza flux tower.

Season	MISR-HR SOS	MISR NEE SOS
1	37,19	39,51
2	42,6	42,61
3	46,9	41,2
4	40,3	38,2
5	41,2	
6	40,6	42,1
7	38,7	40
8	41,5	40,4
9	37,3	39,9
10	37,7	39
11	39,8	36,4
12	35,5	32,9
13	44,4	40,5
14	34,7	31,2
15	32,4	28
16	43,8	43,5
17	36,9	

Table 3.5: MODIS and NEE derived LOS seasonality at the skukuza flux tower.

Season	MODIS LOS	NEE LOS
1	19,78	17,3
2	19,96	21,62
3	18,2	18,66
4	20,28	19,2
5	23,23	22,52

6	17,01	30,49
7	25,8	37,85
8	24,28	8,767
9	29,52	8,731
10	27,27	12,38
11	18,51	18,37
12	33,28	32,4
13	24,03	18,1
14	14,82	20,01
15	27,42	24,51
16	19,64	8,314
17	19,1	10,97

Table 3.6: MISR-HR and NEE derived LOS seasonality at the skukuza flux tower.

Season	MISR-HR LOS	NEE LOS
1	24,85	17,15
2	20,18	23,21
3	20,64	21,2
4	18,96	19,67
5	22,26	
6	21,42	33,24
7	21,34	37,53
8	20,33	18,77
9	31,68	23,33
10	25,3	21,9
11	21,73	19,26
12	28,25	36,13
13	17,29	20,35
14	27,29	20,5
15	31,68	33,21
16	22,2	11,47
17	25,13	

Table 3.7: MODIS and NEE derived EOS seasonality at the skukuza flux tower.

Season	MODIS EOS	NEE EOS
1	57,09	60,8
2	64,6	66,4
3	62,3	67,9
4	60,4	59,8
5	63,1	65,6
6	76	60
7	78,3	63,9
8	51,8	66
9	49,5	71,1
10	51,8	66,7
11	58,7	62,6
12	65,3	68,7

13	59,1	63,7
14	52,7	56,6
15	61,4	69,1
16	52,3	65,3
17	47,8	62,5

Table 3.8: MISR-HR and NEE derived EOS seasonality at the skukuza flux tower.m

Season	MISR-HR EOS	NEE EOS
1	62,04	56,65
2	62,8	65,8
3	67,5	62,4
4	59,2	57,9
5	63,5	
6	62	75,3
7	60	77,5
8	61,9	59,1
9	69	63,2
10	63	60,9
11	61,5	55,7
12	63,7	69
13	61,6	60,8
14	62	51,7
15	64,1	61,2
16	66	55
17	62	

Table 3.9: MODIS and NEE derived POS seasonality at the skukuza flux tower.

Season	MODIS POS	NEE POS
1	46,21	45,38
2	57	51,76
3	59,6	58,8
4	47,1	52,3
5	52,8	43,7
6	48,3	62,3
7	48,4	61,2
8	54,5	47,7
9	54,8	45,1
10	52,5	45,6
11	51,1	52,6
12	49,1	48,7
13	52,6	50,1
14	47,1	47,7
15	51,8	43,8
16	52,7	48,3
17	57,1	46

Table 3.10: MISR-HR and NEE derived POS seasonality at the skukuza flux tower.

Season	MISR_POS	NEE_POS
1	50,4	43,21
2	52,97	51,35
3	56,8	52,5
4	49,8	43,8
5	53,7	
6	50,3	56,1
7	48,6	44,9
8	51,9	46,7
9	55,1	45,8
10	51,5	42,3
11	51	48,3
12	48,3	39,4
13	54,4	44,5
14	49,5	46
15	44,6	43,8
16	57,6	47,3
17	49,2	